**Table 1** Characteristics of 46 neuroblastoma samples

| *Case* | *Type* | *Stage* | *Age (months)* | *MYCN* | *Prognosis* | *p52ShcC* | *p67ShcC* | *p52ShcA* | *p66ShcA* |
|---|---|---|---|---|---|---|---|---|---|
| 1 | I | 1 | 8 | 1 | A | 0.01 | 0 | 0.92 | 0.58 |
| 2 | | 1 | 7 | 1 | A | 0 | 0 | 0.92 | 0.52 |
| 3 | | 1 | 8 | 1 | A | 0.13 | 0.07 | 1.16 | 0.58 |
| 4 | | 1 | 1 | 1 | A | 0 | 0 | 0.81 | 0.63 |
| 5 | | 1 | 4 | 1 | A | 0.013 | 0 | 1.26 | 0.62 |
| 6 | | 1 | 8 | 1 | A | 0.03 | 0.006 | 0.81 | 0.60 |
| 7 | | 1 | 8 | 1 | A | 0 | 0 | 0.54 | 0.70 |
| 8 | | 1 | 7 | 1 | A | 0 | 0 | 0.40 | 0.48 |
| 9 | | 1 | 9 | 1 | A | 0 | 0 | 0.40 | 0.58 |
| 10 | | 1 | 7 | 1 | A | 0.15 | 0.05 | 0.42 | 0.31 |
| 11 | | 1 | 7 | 1 | A | 0.003 | 0 | 0.35 | 0.36 |
| 12 | | 2 | 38 | 1 | A | 0.047 | 0 | 0.41 | 0.20 |
| 13 | | 2 | 7 | 1 | A | 0 | 0 | 0.40 | 0.39 |
| 14 | | 2 | 7 | 1 | A | 0.038 | 0 | 0.60 | 0.63 |
| 15 | | 2 | >132 | 1 | A | 0.03 | 0 | 0.83 | 0.62 |
| 16 | II | 3 | 8 | 1 | A | 0 | 0 | 0.56 | 0.45 |
| 17 | | 3 | 7 | 1 | A | 0.72 | 0.45 | 0.42 | 0.49 |
| 18 | | 3 | 7 | 1 | A | 0.03 | 0.01 | 1.2 | 0.62 |
| 19 | | 3 | 8 | 1 | A | 0.015 | 0.01 | 1.3 | 0.67 |
| 20 | | 3 | 23 | 1 | A | 0 | 0 | 0.25 | 0.32 |
| 21 | | 3 | 22 | 1 | A | 0.10 | 0 | 0.63 | 0.63 |
| 22 | | 3 | >108 | 1 | A | 0.23 | 0.03 | 0.45 | 0.36 |
| 23 | | 3 | 18 | 1 | A | 0.074 | 0.025 | 0.75 | 0.45 |
| 24 | | 3 | 47 | 1 | A* | 0 | 0.03 | 0.87 | 0.65 |
| 25 | | 3 | 21 | 1 | D | 0.089 | 0.03 | 0.76 | 0.56 |
| 26 | | 3 | 96 | 1 | A* | 0.054 | 0.001 | 1.6 | 0.54 |
| 27 | | 4 | 5 | 1 | A | 0.03 | 0 | 1.03 | 0.28 |
| 28 | | 4 | 55 | 1 | A | 0.22 | 0.018 | 1.14 | 0.33 |
| 29 | | 4 | 4 | 1 | A | 0 | 0 | 0.52 | 0.49 |
| 30 | | 4 | 22 | 1 | D | 0.49 | 0.43 | 0.89 | 0.48 |
| 31 | | 4 | 45 | 1 | A* | 0 | 0.068 | 1.17 | 0.53 |
| 32 | | 4 | 57 | 1 | A* | 0.10 | 0.093 | 1.2 | 0.42 |
| 33 | | 4 | 102 | 1 | A* | 0.15 | 0 | 1.5 | 0.49 |
| 34 | III | 3 | 32 | amp | A* | 0 | 0 | 1.6 | 0.37 |
| 35 | | 3 | 13 | amp | D | 0.11 | 0.10 | 0.86 | 0.53 |
| 36 | | 3 | 33 | amp | D | 0.77 | 0.50 | 0.64 | 0.50 |
| 37 | | 3 | 21 | amp | A* | 0.47 | 0.18 | 0.47 | 0.49 |
| 38 | | 3 | 26 | amp | A* | 0.84 | 0.57 | 1.1 | 0.58 |
| 39 | | 4 | 23 | amp | D | 0.38 | 0.13 | 0.99 | 0.35 |
| 40 | | 4 | 7 | amp | D | 0.25 | 0.15 | 1.1 | 0.58 |
| 41 | | 4 | >132 | amp | D | 0.96 | 0.55 | 1.32 | 0.65 |
| 42 | | 4 | 18 | amp | D | 0.22 | 0.13 | 0.99 | 0.63 |
| 43 | | 4 | >24 | amp | D | 0.10 | 0 | 0.76 | 0.54 |
| 44 | | 4 | 59 | amp | D | 0 | 0 | 1.80 | 0.85 |
| 45 | | 4 | 30 | amp | D | 0.99 | 0.76 | 0.60 | 0.56 |
| 46 | | 4 | 34 | amp | D | 0.56 | 0.21 | 0.53 | 0.47 |

Type, as described in 'Materials and methods'; age: onset of the disease (months); stage, INSS stage; MYCN, single copy (1) or amplification (amp) of *MYCN* gene; prognosis, alive (A) or death (D) within 12 months after diagnosis; A*, death after 12 months from diagnosis; p52/p67 ShcC and p52/66 ShcA, the intensity of each band obtained by western analysis, standardized according to control signals, such as the bands of TNB-1 and α-tubulin as described in 'Materials and methods'.

differentiation of TNB-1 cells by knockdown of ShcC was examined. It was found that inhibition of the ERK pathway abolished the neurite outgrowth of TNB-1 cells by ShcC knockdown, indicating that ShcC protein has the potential to suppress neurite outgrowth which is dependent on the sustained activation of the ERK pathway (Figure 3b). In addition, the sustained activation of ERK by the expression of activated Raf protein, RafCAAX (Leevers *et al.*, 1994; Stokoe *et al.*, 1994) also induced neurite outgrowth in TNB-1 cells (Supplementary Figure C) just as in PC12 cells (Dhillon *et al.*, 2003). We also analysed the effect of PI3K inhibitor on neurite outgrowth induced by ShcC RNAi to check the involvement of the PI3K–AKT pathway, whereas no apparent effects on the number and length of the neurite extension were observed (Supplementary Figure D).

*Effect of ShcC knockdown on ERK activation is enhanced by collagen stimulation by ShcA–Grb2 signaling*

Among several culture conditions of cells examined for the effect of ShcC RNAi on the activity of ERK, the most obvious activation of ERK was observed after the

**Table 2** Correlation between the expression of ShcC protein and identified prognostic factors of neuroblastoma

| | *p52* | | *p67* | |
|---|---|---|---|---|
| | *Average* | *t-Test* | *Average* | *t-Test* |
| *ShcC* | | | | |
| *Age (months)* | | | | |
| 12> | 0.071 | | 0.037 | |
| >12 | 0.27 | **<0.001** | 0.18 | 0.015 |
| *Stage* | | | | |
| I–II | 0.03 | | 0.0084 | |
| III–IV | 0.26 | **<0.001** | 0.14 | **<0.001** |
| *MYCN* | | | | |
| Single | 0.083 | | 0.040 | |
| amp. | 0.43 | **0.002** | 0.25 | **0.005** |
| *Death in 12 months* | | | | |
| – | 0.10 | | 0.047 | |
| + | 0.41 | **0.006** | 0.25 | **0.009** |
| | *p52* | | *p66* | |
| | *Average* | *t-Test* | *Average* | *t-Test* |
| *ShcA* | | | | |
| *Age (months)* | | | | |
| 12> | 0.72 | | 0.53 | |
| >12 | 0.82 | 0.2 | 0.52 | 0.32 |
| *Stage* | | | | |
| I–II | 0.68 | | 0.52 | |
| III–IV | 0.82 | 0.1 | 0.52 | 0.22 |
| *MYCN* | | | | |
| Single | 0.73 | | 0.51 | |
| amp. | 0.88 | 0.16 | 0.55 | 0.16 |
| *Death in 12 months* | | | | |
| – | 0.75 | | 0.50 | |
| + | 0.84 | 0.27 | 0.57 | 0.11 |

Expression levels of ShcC and ShcA in tissue samples from 46 neuroblastoma patients quantified were analyzed statistically using *t*-test. The variables compared are age, onset of the disease (months); stage, INSS stage; MYCN, single copy or amplification of *MYCN* gene. Statistically significant correlation ($P<0.01$) is indicated in bold.

cells were plated on collagen dishes following suspending condition (Figure 4a, lower panel). On the contrary, the activation level of ERK due to ShcC RNAi was not significant in the suspending condition (Supplementary Figure E, left panel) showing that ShcC RNAi-induced ERK activation depends on attachment to the specific extracellular matrix (ECM).

In contrast, ERK activation was consistently suppressed by knockdown of ShcA regardless of these culture conditions (Figure 4a, upper panel).

Integrins-mediated extracellular signaling lead the activation of Ras/ERK signaling by ShcA, and that process is reported to be associated with Src family kinase (Wary *et al*., 1996, 1998), focal adhesion kinase (Hecker *et al*., 2002) or some RTKs (Moro *et al*., 1998; Hinsby *et al*., 2004). In TNB-1 cells, enhanced ShcA phosphorylation and ShcA–Grb2 complex formation was observed following collagen stimulation and further increased by ShcC RNAi (Figures 4b and c). To examine whether the phosphorylation of ShcA is necessary for the neurite formation, the effect of double knockdown of both ShcC and ShcA was examined in TNB-1 cells. ERK activation and neurite outgrowth were not detected in the absence of both ShcC and ShcA, indicating that ShcC RNAi-induced neurite outgrowth of TNB-1 cells might be dependent on the ShcA expression in adherent state (Figure 4d).

*Expression of ShcC suppresses the phosphorylation of ShcA in KU-YS cells stimulated by EGF*

To further analyse the effects of ShcC expression on ShcA phosphorylation in neuroblastoma cells, we introduced a vector expressing p52ShcC into KU-YS neuroblastoma cells, which do not express a detectable amount of endogenous ShcC protein (Figure 1A), and obtained several stable clones expressing p52ShcC at different levels (Figure 5a). As controls, clones overexpressing p46/p52ShcA, or expressing the expression vector alone were also prepared. We checked the ShcA phosphorylation of each clone under the stimulation of EGF (Figure 5b). EGF stimulation to the control and ShcA expressing cells showed typical activation of ShcA, whereas the cell expressing ShcC showed decreased levels of ShcA phosphorylation according to the levels of ShcC protein. We also confirmed that activation of ShcA by EGF was suppressed in the cells transiently overexpressing ShcC (Supplementary Figure F). Those cells showed almost the same level of EGF receptor (EGFR) activation induced by EGF, judging from the phosphorylation levels of EGFR indicating that the expression of ShcC negatively affected the EGFR–ShcA signaling after the activation of EGFR, such as competing manners against ShcA. In addition, we examined whether tyrosine phosphorylation of ShcC is crucial for the suppression of ShcA phosphorylation by establishing two clones that express a p52ShcC mutant, 3YF lacking all three tyrosines, which are reported to be involved in the tyrosine phosphorylation of ShcC (Miyake *et al*., 2005). It was revealed that the 3YF mutant of ShcC could suppress the EGF-induced activation of ShcA in both clones almost as efficiently as the original ShcC in ShcC2 cells (Supplementary Figure G), suggesting that negative regulation of ShcA phosphorylation by ShcC does not require tyrosine phosphorylation of ShcC.

*ShcC downregulation negatively affects anchorage-independent growth and* in vivo *tumorigenicity*

We investigated the effect of ShcC knockdown on the anchorage-independent growth and *in vivo* tumorigenicity of TNB-1 cells by establishing cells with stable suppression of ShcC expression using the miR RNAi expression vector (as described in 'Materials and methods'). As analysed in the mixed clones by soft agar colony formation assay, stable suppression of ShcC caused marked inhibition of anchorage-independent growth (Figure 6a). Three isolated clones of ShcC miR

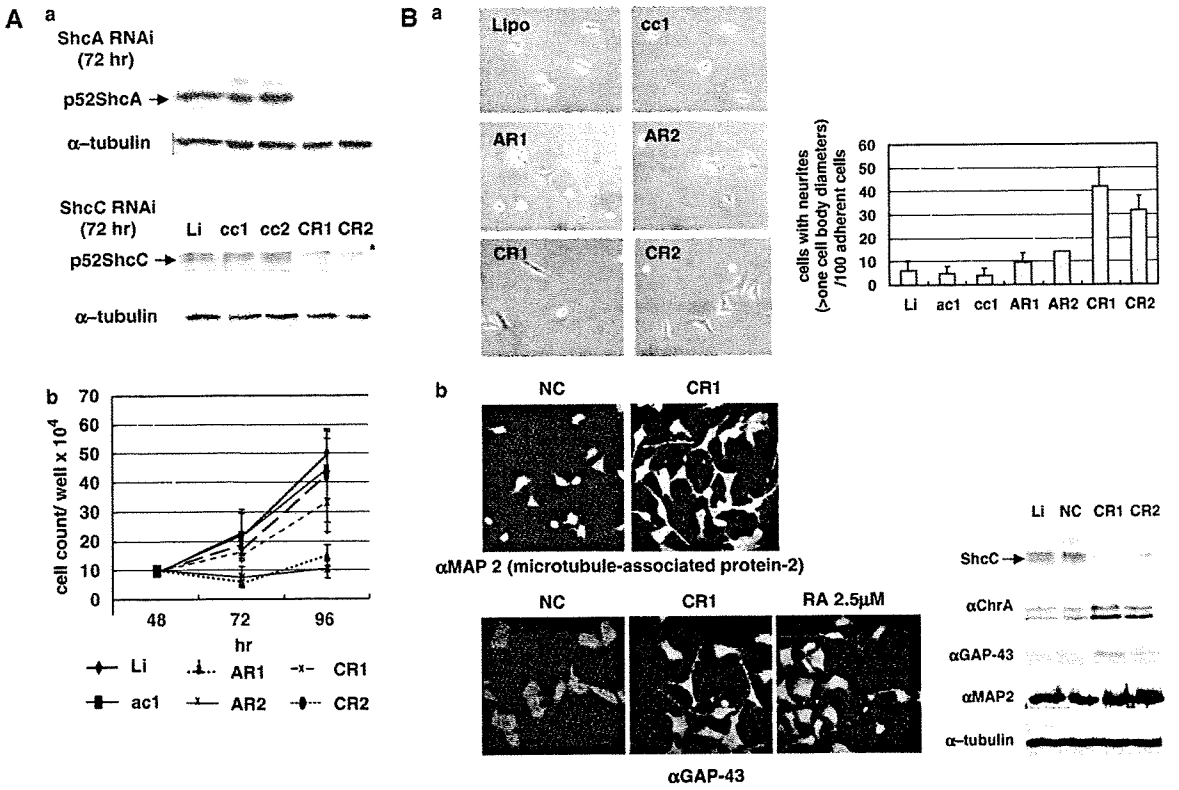


**Figure 2** Biological effects of ShcC downregulation using small interfering RNA (siRNA) on TNB-1 cells. (**A**) (a) Expression of ShcC (lower panel) and ShcA (upper panel) was suppressed by RNA interference using specific siRNA oligonucleotides corresponding to ShcC and ShcA, respectively, then, detected by western analysis with each specific antibody. (b) Growth rate of siRNA-treated cells in tissue culture condition. TNB-1 cells 48 h after the transfection with ShcA/ShcC siRNA cultured by 30-mm dishes were counted at the indicated time points. The results represent the average values (± s.d.) of three replicated experiments. (**B**) Downregulation of ShcC induces neurite outgrowth and increases the expression of differentiation-related markers in TNB-1 cells. (a) Evaluation of neurite outgrowth of ShcA or ShcC-knockdown TNB-1 cells 72 h after siRNA treatment without any extracellular matrix (ECM) stimulation. (b) Expression of several molecules used as differentiation-related markers in ShcC-knockdown TNB-1 cells (left panel: immunostaining of neuritis as described in 'Materials and methods'; right panel: western analysis using indicated antibodies). As a positive control of differentiation, 2.5 μM retinoic acid (RA) was treated 24 h before analysis. AR1, AR2/CR1, CR2: two independent siRNA of ShcA /ShcC; Li: treated with only Lipofectamine 2000; ac1, ac2/cc1, cc2: control siRNA for ShcA /ShcC siRNA, respectively. NC: negative control for universal siRNA (as described in 'Materials and methods').

RNAi (miShcC-1, -2 and -3) were prepared by checking the level of ShcC protein along with clones of LacZ miR RNAi (miLacZ-1 and -2) as controls (Figure 6b). These clones with suppressed level of ShcC showed the same morphological features of neurite formation in tissue culture condition as observed in the cells transfected with ShcC siRNAs (data not shown). The volumes and weights of subcutaneous tumors in nude mice were measured at 6 weeks after injections of the cells and evaluated in at least 4 independent injections per clone. Control LacZ miR RNAi clones (miLacZ-1, miLacZ-2) developed large tumor masses *in vivo* (Figure 6c), whereas remarkable reduction of the size and weight of tumors (or almost disappearance of tumors in some cases) was observed by the stable suppression of ShcC expression. These tumors from ShcC miR RNAi clones showed marked increase in numbers of apoptotic cells compared with control tissues as shown by terminal transferase dUTP nick-end labeling (TUNEL) staining. On the other hand, staining by a proliferation marker, Ki-67 showed no significant difference among each tumor tissue (Figure 6d).

## Discussion

It has already been shown that some signal pathways strongly affect tumor progression and treatment resistance (Schwab *et al.*, 2003). Other than the Trk family, the PI3K/Akt pathway (Opel *et al.*, 2007), Ret (Iwamoto *et al.*, 1993; Marshall *et al.*, 1997), hepatocyte growth factor/c-Met pathway (Hecht *et al.*, 2004) were reported to be closely associated with several diagnostic profiles and biological characteristics of neuroblastoma cells.

This is the first study to show that the expression of ShcC protein, a member of the Shc family docking proteins, is significantly correlated with malignant phenotypes associated with advanced neuroblastoma. Expression of both p52 and p67 isoforms of ShcC,

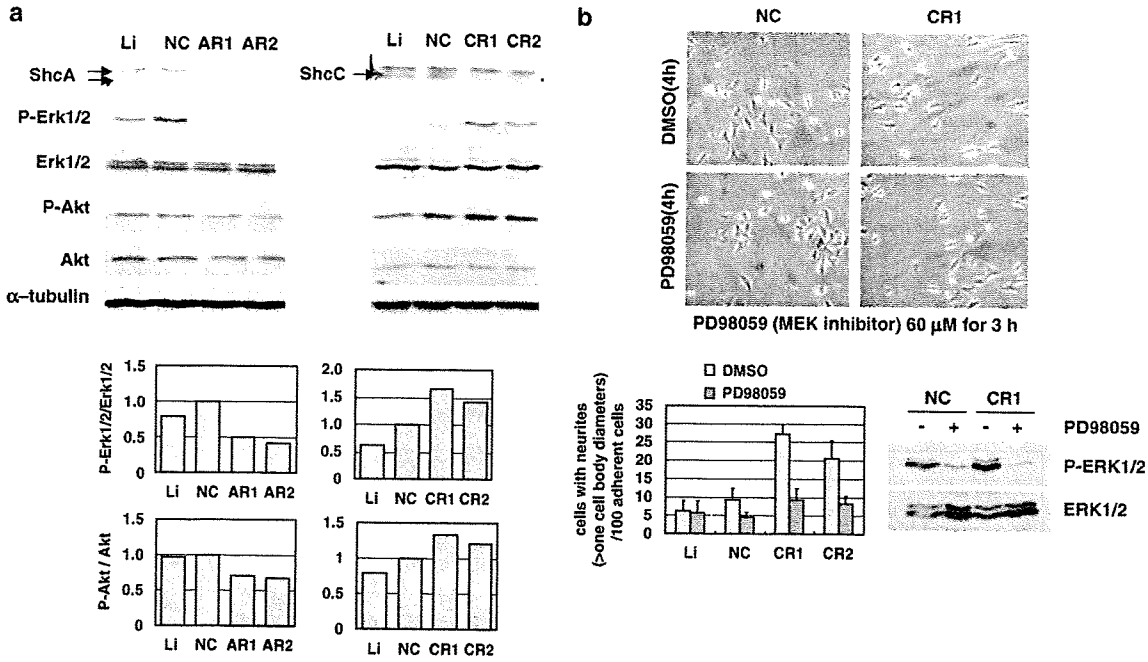


**Figure 3** Persistent activation of extracellular signal-related kinase 1/2 (ERK1/2) in ShcC downregulation induces neurite outgrowth in TNB-1 cells. (**a**) Downregulation of ShcC positively affects the ERK1/2 and Akt pathway in TNB-1 cells. Activation of ERK1/2 and Akt in the cells treated with ShcA or ShcC siRNA were examined by western blotting. The levels of activation were quantified comparing to that of cells treated with control siRNA (NC). (**b**) Effect of MEK inhibitor on neurite outgrowth induced by ShcC RNAi in TNB-1 cells. The siRNA-transfected cells indicated were treated with dimethylsulphoxide (DMSO) or PD98059 and incubated for 3 h in the tissue culture condition, then counted for neurite-containing cells.

shows significant correlation with clinical stage and *MYCN* gene amplification whereas the expression of both isoforms of ShcA, p52 and p66, showed little association with those aspects. These results, in the protein level, give further evidence that ShcC is a factor which determines the prognosis of neuroblastoma, which was recently suggested by analysis of the mRNA expression of ShcC (Terui *et al.*, 2005).

The biological analysis of TNB-1 cells treated with ShcC-specific siRNAs provided evidence that ShcC protein expressed in the neuroblastoma cells is suppressing the differentiation of neuroblastoma cells. Neurite outgrowth of TNB-1 cells, induced by downregulation of ShcC was dependent on sustained activation of the MEK/ERK pathway. Sustained activation of the ERK pathway triggered by factors such as NGF is required for neuronal differentiation in some neuronal tumor cells such as PC12 cells (Qui and Green, 1992; Yaka *et al.*, 1998). The fact that constitutively activated Raf–ERK signaling induced neurite outgrowth in the same cell line (Supplementary Figure C), such as the RTK-related pathway might induce the ERK activation and cellular differentiation in TNB-1 cells, although NGF stimulation failed to induce neurite elongation of TNB-1 cells (data not shown).

Interestingly, elevation in the level of phosphorylated ShcA followed by activation of the ERK pathway by ShcA–Grb2 signals was observed in TNB1 when the ShcC protein expression was suppressed by RNAi. This activation of the ShcA–Grb2–ERK pathway caused by downregulation of ShcC may be due to a competitive effect between ShcC and ShcA for binding to certain RTKs. This possibility is supported by another experiment showing that both EGF-induced phosphorylation of ShcA and complex formation between ShcA and Grb2 in KU-YS cells are suppressed by the expression of ShcC in a dose-dependent manner. It was shown that the expression of the PTB domains of ShcC partially interfered with the binding of endogenous ShcA to activated EGFR in 293 cells (O'Bryan *et al.*, 1998). These data are consistent with our current findings described above. It is suspected that some types of differentiation signals mediated by ShcA are blocked by the overexpression of ShcC in some neuroblastoma cells such as TNB-1, and the suppression of ShcC protein by RNAi causes the ShcA-mediated differentiation of these cells.

Elevated level of ShcA phosphorylation and ERK activation induced by ShcC downregulation was more significant under the stimulation of collagen I than without any ECM stimulation. In addition, in suspending condition we could not detect any activation of ShcA nor ERK signal after ShcC downregulation (Supplementary Figure E). These results indicate that the difference between ShcA and ShcC might be in interaction with matrix-adhesion signals. ShcA is considered to be implicated in the adherent related pathway, phosphorylated by forming a complex with

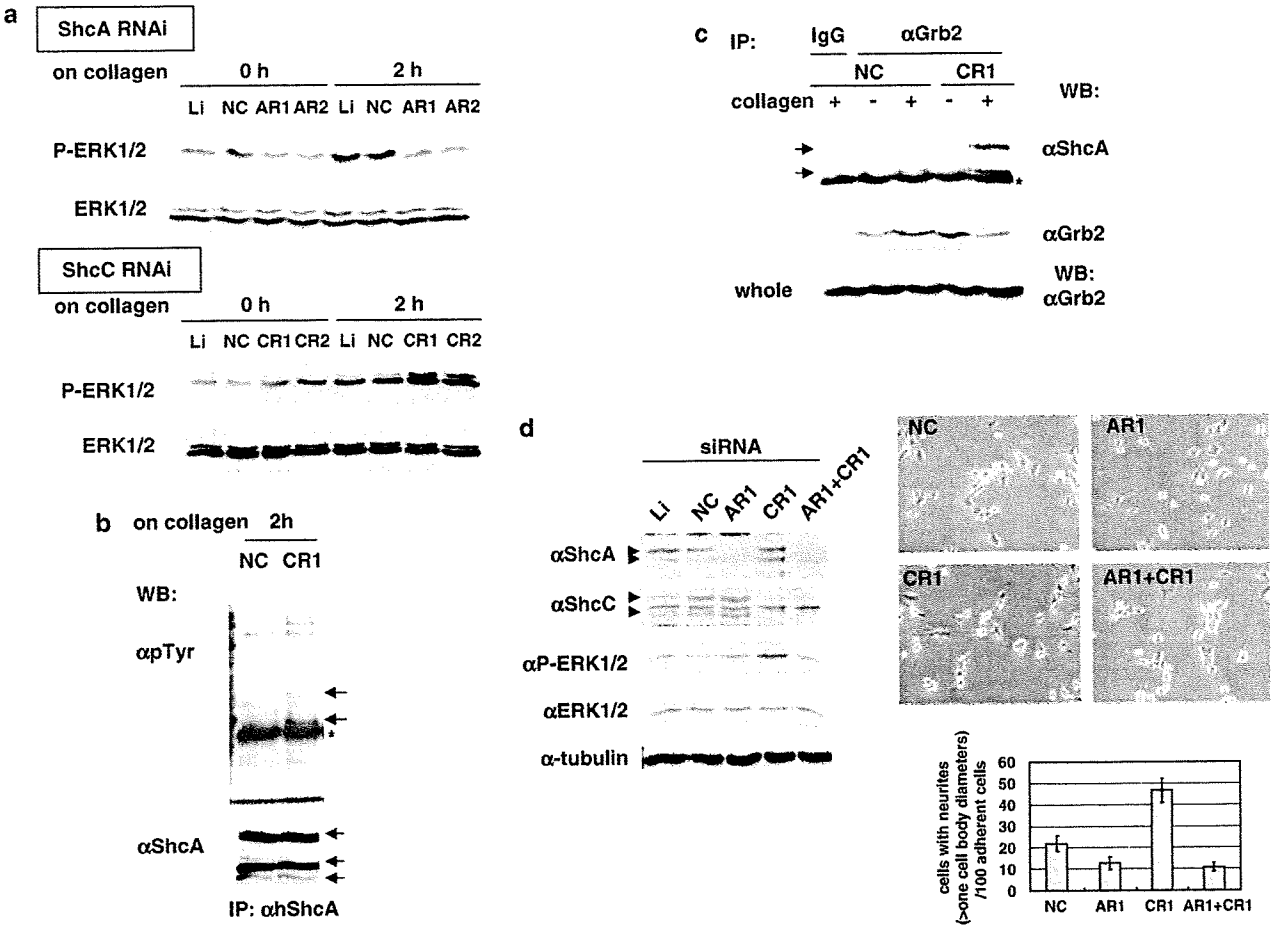


**Figure 4** Elevation of extracellular signal-regulated kinase ()-activated level in ShcC-knockdown cells is increased by collagen stimulation by ShcA–Grb2 signaling. (**a**) Elevation of the ERK1/2-activated level due to ShcC downregulation is further increased 2 h after collagen stimulation. siRNAs of ShcA/ShcC-transfected TNB-1 cells (AR1, AR2/CR1, CR2, respectively) were incubated in the tissue culture condition for 70 h and stimulated by collagen type I. Duplicated cells were harvested 0 and 2 h after collagen stimulation (as described in 'Materials and methods'). (**b**) After collagen stimulation ShcA was phosphorylated more strongly in ShcC-knockdown cells than the control cells. Asterisks show heavy chains of immunoglobulin. (**c**) ShcA–Grb2 complex formation (upper panel) were increased by downregulation of ShcC. (**d**) The ShcA-knockdown effect on the neurite outgrowth in cells transfected with ShcC siRNA was evaluated by the same method performed in Figure 2Ba. The number of neurites observed in the cells transfected with both ShcA and ShcC siRNA was obviously decreased compared to cells transfected with only ShcC siRNA.

Fyn (Wary *et al.*, 1998) through its proline-rich region that is not conserved in ShcC.

In tissue culture and in transgenic mice, signaling through Fyn has been closely associated with neurite extension and cell adhesion (Brouns *et al.*, 2000, 2001). Berwanger *et al.* (2002) referred to the inverse correlation between the expression of Fyn and progression of neuroblastoma from 94 primary neuroblastoma specimens, showing that expressed Fyn-induced differentiation and growth arrest of neuroblastoma cell lines. Another report indicated that active Fyn kinase induces a lasting activation of the MAPK pathway through inhibition of MAPK phosphatase 1 (Wellbrock *et al.*, 2002). We confirmed that neurite outgrowth of ShcC-knockdown TNB-1 cells was suppressed by Src family inhibitor, PP2 (Supplementary Figure H). These data suggest the possibility that Integrin–Fyn–ShcA signals could be closely associated with the differentiation of TNB-1 cells induced by ShcC downregulation along with the signals of RTK–ShcA/ShcC.

Noticeably, the interference of the ShcA-mediated signaling by ShcC protein is independent of tyrosine phosphorylation of ShcC. The function of the nonphosphorylated domain of ShcC such as SH2 might be also highlighted. As for the difference in the downstream signaling between ShcC and ShcA, little is known so far. Regarding to this point, Nakamura *et al.* (2002) indicated that inhibition of NGF-induced ERK activation by the expression of ShcC was due to the different Grb2-binding capacity between ShcA and ShcC in response to NGF. It was previously reported that ShcA preferentially binds to TrkA (Yamada *et al.*, 2002), which is the key receptor against NGF due to neurite outgrowth with the sustained ERK phosphorylation,

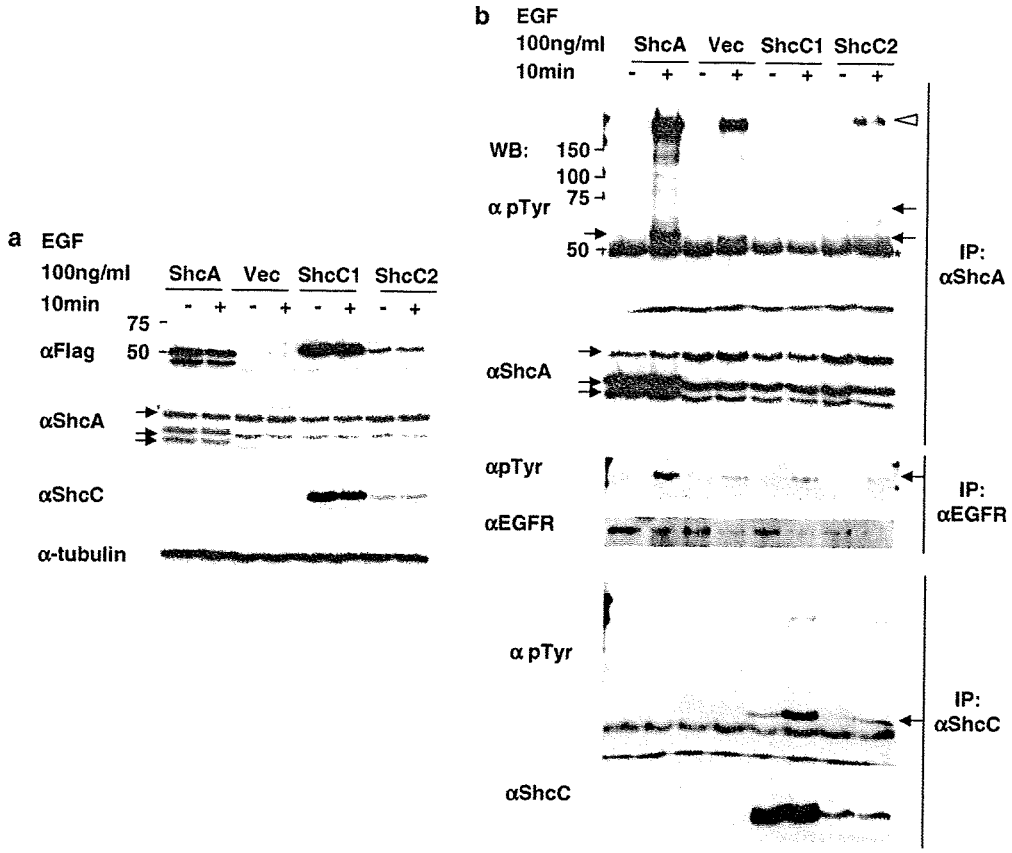


**Figure 5** High expression of ShcC suppresses the phosphorylation of ShcA in KU-YS cells stimulated by epidermal growth factor (EGF). We generated stable clones of KU-YS cells expressing Flag-tagged ShcA and diverse levels of p52ShcC (ShcC1 and ShcC2) other than clones transfected with the control vector. (**a**) Each expression level was detected by western analysis. (**b**) Levels of expression and tyrosine phosphorylation of EGFR (middle panel), ShcA (upper panel) and ShcC (lower panel) were analysed by immunoprecipitation and immunoblotting using the antibodies indicated in figure in the KU-YS clone cells stimulated by EGF (as described in 'Materials and methods'). Asterisks show heavy chains of immunoglobulin.

whereas ShcC associated with TrkB rather than TrkA (O'Bryan *et al.*, 1998; Liu and Meakin, 2002). In neuroblastoma, the function of signal pathways downstream of these two neurotrophin receptors might be quite different (Nakagawara *et al.*, 1993), also suggesting the distinct function of downstream signal mediated by ShcC.

The effect of ShcC knockdown in *in vivo* tumorigenicity was quite remarkable comparing the effect in growth rate in tissue culture condition. We found that anchorage-independent growth in cells was also dramatically decreased by knockdown of ShcC as shown by soft agar assay (Figure 6a). Furthermore, the proportion of apoptotic cells in the nude mouse tumors generated from neuroblastoma cells *in vivo* was remarkably increased by the knockdown of ShcC. In recent study, Magrassi *et al.* (2005) showed that ShcC positively effects on cell survival by PI3K–AKT pathway in glioma cells using dominant negative form of ShcC. Theses data indicate that ShcC has additional function in the protection from some types of apoptosis in addition to the induction of differentiation of cells.

It was indicated that ShcC might have a potent function for tumor progression in neuroblastoma by suppressing the differentiation and by promoting the anchorage-independent growth in the majority of neuroblastoma cells which has high expression of ShcC protein. From these points of view, we suggest that ShcC is a potent tool for predicting the phenotype of neuroblastoma and is also a good candidate for therapeutic targets of advanced neuroblastoma.

## Materials and methods

### *Cell culture and tissue samples*

DLD-1 cells and all cell lines of neuroblastomas in this study were prepared as described in the previous report (Miyake *et al.*, 2002). These cells were cultured in an RPMI 1640 medium with 10% fetal calf serum (FCS) (Sigma, St Louis, MO, USA) at 37 °C in an atmosphere containing 5% $CO_2$.

Anonymous 46 frozen neuroblastoma tissues were used in this study. The samples were divided into three subsets using Brodeur's classification; type I (stage 1, 2 or 4S; a single copy of *MYCN*), type II (stage 3 or 4; a single copy of *MYCN*) and type III (all stages; amplification of *MYCN*) (Brodeur and Nakagawara, 1992; Ohira *et al.*, 2003). A total of 15 samples belonged to type I, 18 samples to type II and 13 samples to type III. Staging classification was according to the

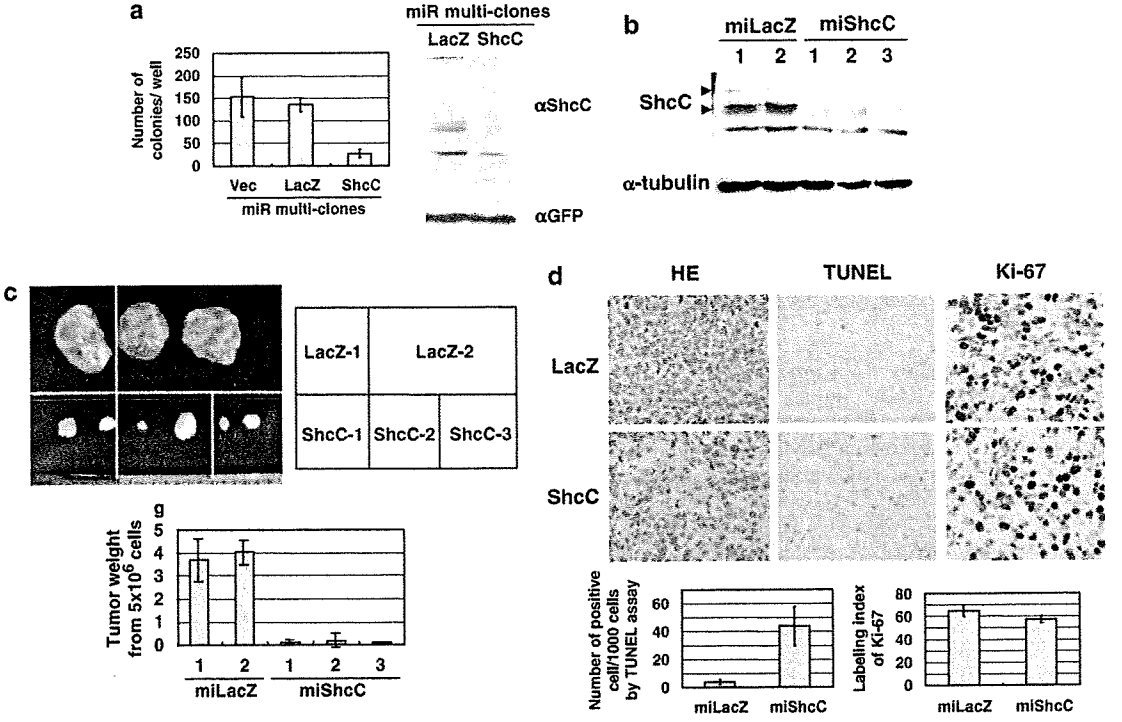


**Figure 6** ShcC downregulation negatively affects tumorigenicity *in vivo*. (**a**) Cells transfected with the miR RNAi vector for ShcC (miShcC) and LacZ (miLacZ) that also contains an EmGFP coding sequence for co-cistronic expression with the pre-miRNA were cultured in medium containing blasticidin (Invivogen) for only 1 week, and then mixed. Multiclone cells for LacZ and ShcC were analysed for the ability of anchorage-independent growth using soft agar assay by $1 \times 10^4$ cells per a well of six-well plate for 3 weeks (as described in previous report: Miyake *et al*., 2005). The results represent the average value (± s.d.) of three replicated experiments. (**b**) Expression levels of ShcC in clones of TNB-1 cells stably transfected with miR RNAi expression vector for LacZ (miLacZ-1 and miLacZ-2) and ShcC (miShcC-1, -2 and -3) were detected by western analysis using αhShcC (as described in 'Materials and methods'). (**c**) Nude mouse tumors derived from two clones of LacZ miR RNAi and three clones of ShcC. Upper panel: Photographs of tumors from nude mice at 6 weeks after subcutaneous injections of $5 \times 10^6$ cloned cells (bar: 20 mm); lower panel: ability of *in vivo* tumorigenicity is shown by average weight (±) of four tumor derived from each clone. (**d**) ShcC-knockdown cells show tendency to apoptosis *in vivo*. Upper panel: Photographs of a cross-section of each tumor tissues from miLacZ-1 and miShcC-2 using microscope at a magnification of ×400, that were stained with hematoxylin and eosin (HE), diaminobenzidine (DAB) by terminal transferase dUTP nick-end labeling (TUNEL) assay and anti-Ki-67 antibody (bar: 25 μm); lower panel: the tendency to apoptosis was defined as the number of positive stained cells per 1000 tumor cells in TUNEL assay and the proliferating activity was indicated as the labeling index of Ki-67 by counting 1000 tumor cells. The data show the average scores ± s.d. of positive cells in three different areas of each slide. Staining of each sample was owing to the procedure by SRL Inc.

International Neuroblastoma Staging System and *N-Myc* amplification (> 10 copy) accepted as a poor prognostic risk factor was checked before clinical intervention.

*Reagents*

The polyclonal antibodies against the CH1 domain of human ShcC (amino acid 225–324):αhShcC were generated by the same method as described previously (Miyake *et al*., 2002). Polyclonal antibodies of human ShcA:αhShcA were prepared as described in previous reports (Miyake *et al*., 2002).

Other antibodies were purchased as follows: antiphosphotyrosine antibody (4G10) (Upstate Biotechnology Inc., Charlottesville, VA, USA), anti-ShcA/ShcC monoclonal antibodies: αShcA/αShcC (BD Transduction Laboratories, San Diego, CA, USA), anti-α-tubulin antibody (Zymed Laboratories, San Francisco, CA, USA), anti-p44/42 MAPK (ERK1/2), antiphospho-p44/42 MAPK (P-ERK1/2), anti-Akt, and antiphospho-Akt (Ser473) (P-Akt) antibodies (Cell Signaling, Danvers, MA, USA), anti-chromogranin A (ChrA) antibody (Santa Cruz Biotechnology, Santa Cruz, CA, USA), anti-GAP43 antibody (Zymed Laboratories), anti-MAP2 antibody (Santa Cruz Biotechnology), anti-c-Src antibody (Upstate Biotechnology Inc.), anti-phospho-Src family antibody (Tyr416) (Cell Signaling), anti-Grb2 antibody (BD Transduction Laboratories), anti-T7tag antibody (Novagen, San Diego, CA, USA) and anti-Flag M2 antibody (Sigma). As secondary antibodies, horseradish peroxidase-conjugated anti-rabbit and anti-mouse IgGs (GE Healthcare, Buckinghamshire, UK) were used. All inhibitors used in this study (PD98059, LY294002, PP2 and PP3) were purchased from Calbiochem, San Diego, CA, USA.

*Cell stimulation, immunoprecipitation and immunoblotting*

Cell stimulation analysis with EGF (Wako) was performed as described (Miyake *et al*., 2002). The cells were starved for 24 h and treated for 5 min with EGF (100 ng/ml). As for stimulation with collagen type I, cultured cells with or without serum for 24 h were detached from culture dishes by pipette treatment and after the suspending condition for 30 min, seeded onto a collagen type I-coated dish (Iwaki, Tokyo, Japan). Cells were harvested after 2 h using PLC lysis buffer. Control cells were harvested before the attachment on the collagen I-coated

surface. The immunoprecipitation and western analysis were performed using the procedure described in a previous report (Miyake *et al.*, 2002).

*Quantification and statistical analysis of expression levels of ShcC/ShcA*

The intensity of each band obtained by western analysis was measured using a molecular imager (GS-800; Bio-Rad, Hercules, CA, USA) and standardized according to control signals, such as the bands of TNB-1 and α-tubulin.

*t*-Test performed by Excel was used to evaluate the significance of the two groups quantified expression levels of indicated molecules.

*Knockdown of ShcA/ShcC by RNA interference*

For siRNAs, Stealth RNA duplex oligoribonucleotides (Invitrogen, Carlsbad, CA, USA) was used to knockdown ShcC/ShcA protein. The following two 25-mer oligonucleotide pairs for each molecule were available. As for ShcC, CR1: 5′-GCUGGCCAAAGCGCUCUAUGACAAU-3′ (nucleotides 141–165), CR2: 5′-CCAAGAUCUUUGUGGCGCACA GCAA-3′ (nucleotides 2447–2471). As negative controls for each oligonucleotide pair, cc1: GGCUCCAGAACGGCCUUAGU AACAU-3′, cc2: GGAAACCGACAACUACGAUGUCAAU, respectively. As for ShcA, AR1: 5′-GGAGUAACCUGAA AUUUGCUGGAAU-3′ (nucleotides 335–359). AR2: 5′-GCCU UCGAGUUGCGCUUCAAACAAU-3′ (nucleotides 689–611). As a negative control for each, ac1: GGAAACCGUAAUAUU CGGUGUGAA, ac2: 5′-UGCCGCGAUUCGCGUUACAAC UUAAU, respectively. As the other negative control for universal siRNA, Stealth RNAi Negative Control Duplexes (Medium GC Duplex) (Invitrogen) was used (NC). Cells were transfected with siRNA using Lipofectamine 2000 (Invitrogen) according to the manufacturer's instructions. Cells ($5 \times 10^5$ per well of a six-well plate) in suspending condition were transfected twice at 24 h interval (5 μl of 20 μM siRNA each) and analysed 48 h after second transfection.

A system stably expressing miRNA was generated using the BLOCK-iT Pol II miR RNAi Expression Vector Kit with EmGFP (Invitrogen) according to the manufacturer's instructions. In the generation of the miR RNAi vector for humans, ShcC was chosen as the target sequence, using the top/bottom oligo sequence: 5′-TGCTGCTTGGAGGCTTTCTCTTCTT GGTTTTGGCCACTGACTGACCAAGAAGAAAGCCTC CAAG-3′/5′-CCTGCTTGGAGGCTTTCTTCTTGGTCAGTC AGTGGCCAAAACCAAGAAGAGAAAGCCTCCAAGC-3′. Cells stably expressing the miR RNAi vector for ShcC (miShcC) and LacZ (miLacZ), that were also expressing green fluorescent protein were established and cultured in medium containing blasticidin (InvivoGen, San Diego, CA, USA) at a concentration of 15 μg/ml for 3 weeks. Three clones expressing the ShcC RNAi vector were selected by significant suppression of the ShcC protein (< 10%), and two clones from the control LacZ vector were also selected. Cells transfected with miR-negative control plasmid (one of kit components) were used as other control cells (Vec).

*Generation of KU-YS cells stably expressing ShcA/ShcC*

The full-length human ShcA cDNA for transfection was donated by Dr N Goto. ShcA and ShcC cDNAs were inserted with C-terminal Flag epitope tag into a mammalian expression vector pcDNA3.1A. All parts amplified by PCR were verified by sequencing. The stable expression of the full-length of ShcA and full-length of ShcC in KU-YS cells were obtained by transfection using transfection reagent Lipofectamine 2000 (Invitrogen) according to the manufacturer's instructions. The KU-YS cells transfected with pcDNA3.1 vector (mock) were used as a control. Then, cells were selected according to the method described previously and the expression level of each independent clone was evaluated by immunoblotting analysis.

**Acknowledgements**

This work was supported by a Grant-in-Aid from the Ministry of Health, Labor and Welfare of Japan for the third-term Comprehensive 10-year Strategy for Cancer Control.

**References**

Berwanger B, Hartmann O, Bergmann E, Bernard S, Nielsen D, Krause M *et al.* (2002). Loss of a FYN-regulated differentiation and growth arrest pathway in advanced stage neuroblastoma. *Cancer Cell* **2**: 377–386.

Brodeur GM, Nakagawara A. (1992). Molecular basis of clinical heterogeneity in neuroblastoma. *Am J Pediatr Hematol Oncol* **14**: 111–116.

Brouns MR, Matheson SF, Hu KQ, Delalle I, Caviness VS, Silver J *et al.* (2000). The adhesion signaling molecule p190 RhoGAP is required for morphogenetic processes in neural development. *Development* **127**: 4891–4903.

Brouns MR, Matheson SF, Settleman J. (2001). p190 RhoGAP is the principal Src substrate in brain and regulates axon outgrowth, guidance and fasciculation. *Nat Cell Biol* **3**: 361–367.

Dhillon AS, Meikle S, Peyssonnaux C, Grindlay J, Kaiser C, Steen H *et al.* (2003). A Raf-1 mutant that dissociates MEK/extracellular signal-regulated kinase activation from malignant transformation and differentiation but not proliferation. *Mol Cell Biol* **23**: 1983–1993.

Giudici AM, Sher E, Pelagi M, Clementi F, Zanini A. (1992). Immunolocalization of secretogranin II, chromogranin A, and chromogranin B in differentiating human neuroblastoma cells. *Eur J Cell Biol* **58**: 383–389.

Hecht M, Papoutsi M, Tran HD, Wilting J, Schweigerer L. (2004). Hepatocyte growth factor/c-Met signaling promotes the progression of experimental human neuroblastomas. *Cancer Res* **64**: 6109–6118.

Hecker TP, Grammer JR, Gillespie GY, Stewart Jr J, Gladson CL. (2002). Focal adhesion kinase enhances signaling through the Shc/extracellular signal-regulated kinase pathway in anaplastic astrocytoma tumor biopsy samples. *Cancer Res* **62**: 2699–2707.

Hinsby AM, Lundfald L, Ditlevsen DK, Korshunova I, Juhl L, Meakin SO *et al.* (2004). ShcA regulates neurite outgrowth stimulated by neural cell adhesion molecule but not by fibroblast growth factor 2: evidence for a distinct fibroblast growth factor receptor response to neural cell adhesion molecule activation. *J Neurochem* **91**: 694–703.

Iwamoto T, Taniguchi M, Wajjwalku W, Nakashima I, Takahashi M. (1993). Neuroblastoma in a transgenic mouse carrying a metallothionein/ret fusion gene. *Br J Cancer* **67**: 504–507.

Leevers SJ, Paterson HF, Marshall CJ. (1994). Requirement for Ras in Raf activation is overcome by targeting Raf to the plasma membrane. *Nature* **369**: 411–414.

Liu HY, Meakin SO. (2002). ShcB and ShcC activation by the Trk family of receptor tyrosine kinases. *J Biol Chem* **277**: 26046–26056.

Magrassi L, Conti L, Lanterna A, Zuccato C, Marchionni M, Cassini P *et al.* (2005). Shc3 affects human high-grade astrocytomas survival. *Oncogene* **24**: 5198–5206.

Marshall GM, Peaston AE, Hocker JE, Smith SA, Hansford LM, Tobias V *et al.* (1997). Expression of multiple endocrine neoplasia 2B RET in neuroblastoma cells alters cell adhesion *in vitro*, enhances

metastatic behavior *in vivo*, and activates Jun kinase. *Cancer Res* **57**: 5399–5405.

Miyake I, Hakomori Y, Misu Y, Nakadate H, Matsuura N, Sakamoto M *et al.* (2005). Domain-specific function of ShcC docking protein in neuroblastoma cells. *Oncogene* **24**: 3206–3215.

Miyake I, Hakomori Y, Shinohara A, Gamou T, Saito M, Iwamatsu A *et al.* (2002). Activation of anaplastic lymphoma kinase is responsible for hyperphosphorylation of ShcC in neuroblastoma cell lines. *Oncogene* **21**: 5823–5834.

Moro L, Venturino M, Bozzo C, Silengo L, Altruda F, Beguinot L *et al.* (1998). Integrins induce activation of EGF receptor: role in MAP kinase induction and adhesion-dependent cell survival. *EMBO J* **17**: 6622–6632.

Nakagawara A, Arima-Nakagawara M, Scavarda NJ, Azar CG, Cantor AB, Brodeur GM. (1993). Association between high levels of expression of the TRK gene and favorable outcome in human neuroblastoma. *N Engl J Med* **328**: 847–854.

Nakagawara A, Brodeur GM. (1997). Role of neurotrophins and their receptors in human neuroblastomas: a primary culture study. *Eur J Cancer* **33**: 2050–2053.

Nakamura T, Komiya M, Gotoh N, Koizumi S, Shibuya M, Mori N. (2002). Discrimination between phosphotyrosine-mediated signaling properties of conventional and neuronal Shc adapter molecules. *Oncogene* **21**: 22–31.

Nakamura T, Muraoka S, Sanokawa R, Mori N. (1998). N-Shc and Sck, two neuronally expressed Shc adapter homologs. Their differential regional expression in the brain and roles in neurotrophin and Src signaling. *J Biol Chem* **273**: 6960–6967.

Nakamura T, Sanokawa R, Sasaki Y, Ayusawa D, Oishi M, Mori N. (1996). N-Shc: a neural-specific adapter molecule that mediates signaling from neurotrophin/Trk to Ras/MAPK pathway. *Oncogene* **13**: 1111–1121.

O'Bryan JP, Lambert QT, Der CJ. (1998). The src homology 2 and phosphotyrosine binding domains of the ShcC adaptor protein function as inhibitors of mitogenic signaling by the epidermal growth factor receptor. *J Biol Chem* **273**: 20431–20437.

O'Bryan JP, Songyang Z, Cantley L, Der CJ, Pawson T. (1996). A mammalian adaptor protein with conserved Src homology 2 and phosphotyrosine-binding domains is related to Shc and is specifically expressed in the brain. *Proc Natl Acad Sci USA* **93**: 2729–2734.

Ohira M, Morohashi A, Inuzuka H, Shishikura T, Kawamoto T, Kageyama H *et al.* (2003). Expression profiling and characterization of 4200 genes cloned from primary neuroblastomas: identification of 305 genes differentially expressed between favorable and unfavorable subsets. *Oncogene* **22**: 5525–5536.

Opel D, Poremba C, Simon T, Debatin KM, Fulda S. (2007). Activation of Akt predicts poor outcome in neuroblastoma. *Cancer Res* **67**: 735–745.

Osajima-Hakomori Y, Miyake I, Ohira M, Nakagawara A, Nakagawa A, Sakai R. (2005). Biological role of anaplastic lymphoma kinase in neuroblastoma. *Am J Pathol* **167**: 213–222.

Pelicci G, Dente L, De Giuseppe A, Verducci-Galletti B, Giuli S, Mele S *et al.* (1996). A family of Shc related proteins with conserved PTB, CH1 and SH2 regions. *Oncogene* **13**: 633–641.

Qui MS, Green SH. (1992). PC12 cell neuronal differentiation is associated with prolonged p21ras activity and consequent prolonged ERK activity. *Neuron* **9**: 705–717.

Ravichandran KS. (2001). Signaling via Shc family adapter proteins. *Oncogene* **20**: 6322–6330.

Sakai R, Henderson JT, O'Bryan JP, Elia AJ, Saxton TM, Pawson T. (2000). The mammalian ShcB and ShcC phosphotyrosine docking proteins function in the maturation of sensory and sympathetic neurons. *Neuron* **28**: 819–833.

Schwab M, Westermann F, Hero B, Berthold F. (2003). Neuroblastoma: biology and molecular and chromosomal pathology. *Lancet Oncol* **4**: 472–480.

Stokoe D, Macdonald SG, Cadwallader K, Symons M, Hancock JF. (1994). Activation of Raf as a result of recruitment to the plasma membrane. *Science* **264**: 1463–1467.

Terui E, Matsunaga T, Yoshida H, Kouchi K, Kuroda H, Hishiki T *et al.* (2005). Shc family expression in neuroblastoma: high expression of shcC is associated with a poor prognosis in advanced neuroblastoma. *Clin Cancer Res* **11**: 3280–3287.

Wary KK, Mainiero F, Isakoff SJ, Marcantonio EE, Giancotti FG. (1996). The adaptor protein Shc couples a class of integrins to the control of cell cycle progression. *Cell* **87**: 733–743.

Wary KK, Mariotti A, Zurzolo C, Giancotti FG. (1998). A requirement for caveolin-1 and associated kinase Fyn in integrin signaling and anchorage-dependent cell growth. *Cell* **94**: 625–634.

Wellbrock C, Weisser C, Geissinger E, Troppmair J, Schartl M. (2002). Activation of p59(Fyn) leads to melanocyte dedifferentiation by influencing MKP-1-regulated mitogen-activated protein kinase signaling. *J Biol Chem* **277**: 6443–6454.

Yaka R, Gamliel A, Gurwitz D, Stein R. (1998). NGF induces transient but not sustained activation of ERK in PC12 mutant cells incapable of differentiating. *J Cell Biochem* **70**: 425–432.

Yamada M, Numakawa T, Koshimizu H, Tanabe K, Wada K, Koizumi S *et al.* (2002). Distinct usages of phospholipase C gamma and Shc in intracellular signaling stimulated by neurotrophins. *Brain Res* **955**: 183–190.

Supplementary Information accompanies the paper on the Oncogene website (http://www.nature.com/onc)

JEM

ARTICLE

# Netrin-1 acts as a survival factor for aggressive neuroblastoma

Céline Delloye-Bourgeois,[1] Julien Fitamant,[1] Andrea Paradisi,[1] David Cappellen,[2] Setha Douc-Rasy,[2] Marie-Anne Raquin,[3] Dwayne Stupack,[4] Akira Nakagawara,[5] Raphaël Rousseau,[6] Valérie Combaret,[6] Alain Puisieux,[6] Dominique Valteau-Couanet,[3] Jean Bénard,[2] Agnès Bernet,[1] and Patrick Mehlen[1]

[1]Apoptosis, Cancer and Development Laboratory, Equipe labellisée 'La Ligue', Centre National de la Recherche Scientifique UMR5238, Université de Lyon, 69008 Lyon, France
[2]Molecular Interactions and Cancer Centre, National de la Recherche Scientifique UMR 8126 and IFR54, and [3]Oncopediatric Department, Gustave Roussy Institute, 94805 Villejuif Cedex, France
[4]Department of Pathology, School of Medicine, Moores Cancer Center, University of California, San Diego, La Jolla, CA 92093
[5]Division of Biochemistry, Chiba Cancer Center Research Institute, Chiba 260-8717, Japan
[6]Institut National de la Santé et de la Recherche Médicale U590, Unité d'Oncologie Moléculaire, Université de Lyon, 69008 Lyon, France

**Neuroblastoma (NB), the most frequent solid tumor of early childhood, is diagnosed as a disseminated disease in >60% of cases, and several lines of evidence support the resistance to apoptosis as a prerequisite for NB progression. We show that autocrine production of netrin-1, a multifunctional laminin-related molecule, conveys a selective advantage in tumor growth and dissemination in aggressive NB, as it blocks the proapoptotic activity of the UNC5H netrin-1 dependence receptors. We show that such netrin-1 up-regulation is a potential marker for poor prognosis in stage 4S and, more generally, in NB stage 4 diagnosed infants. Moreover, we propose that interference with the netrin-1 autocrine loop in malignant neuroblasts could represent an alternative therapeutic strategy, as disruption of this loop triggers in vitro NB cell death and inhibits NB metastasis in avian and mouse models.**

CORRESPONDENCE
Patrick Mehlen:
mehlen@lyon.fnclcc.fr

Abbreviations used: CAM, chorioallantoic membrane; DAPK, DAP kinase; DCC, deleted in colorectal cancer; MNA, *MYCN* amplification; mRNA, messenger RNA; Myoc, myocardium; NB, neuroblastoma; PTX, primary tumor xenograft; Q-RT-PCR, quantitative RT-PCR; siRNA, small interfering RNA; TUNEL, terminal deoxynucleotidyl transferase–mediated dUTP-biotin nick end labeling.

Dependence receptors now number more than a dozen, including deleted in colorectal cancer (DCC) (1), UNC5H (2), Patched (3), some integrins (4), neogenin (5), $p75^{NTR}$ (6), RET (7), ALK (8), and TrkC (9). Although they have no structural homology (other than possibly in a domain referred to as the DART [dependence-associated receptor transmembrane] domain) (10), they all share the functional property of inducing cell death when disengaged from their trophic ligands, whereas the presence of their trophic ligands blocks this proapoptotic activity. Such receptors thus create cellular states of dependence on their respective ligands (11, 12).

The prototype dependence receptors are the netrin-1 receptors. Netrin-1, a diffusible laminin-related protein, has been shown to play a major role in the control of neuronal navigation during the development of the nervous system by interacting with its main receptors, DCC (13, 14, 15) and UNC5H (16, 17). However, DCC and UNC5H (i.e., UNC5H1, UNC5H2, UNC5H3, and UNC5H4) have been shown to belong to the dependence receptor family (1, 2). This dependence effect upon netrin-1 has been suggested to act as a mechanism for eliminating tumor cells that would develop in settings of ligand unavailability (for reviews see references 18, 19). Along this line, disruption of the proapoptotic signaling of these netrin-1 receptors in the gastrointestinal tracts of mice, by netrin-1 overexpression or by inactivation of UNC5H3, is associated with intestinal tumor progression (20, 21).

Thus, loss of the dependence receptors' proapoptotic activity represents a selective advantage for tumor cells. In this respect, DCC was proposed in the early 1990s to function as a tumor suppressor gene, whose expression is lost in

J. Bénard, A. Bernet, and P. Mehlen contributed equally to this paper.



The Rockefeller University Press $30.00
J. Exp. Med. Vol. 206 No. 4 833-847
www.jem.org/cgi/doi/10.1084/jem.20082299





The Journal of Experimental Medicine

the vast majority of human cancers (22, 23). This hypothesis also fits with the observation that UNC5H genes are down-regulated in most colorectal tumors, hence suggesting that loss of UNC5H genes represents a selective advantage for tumor development (21, 24, 25). We have analyzed expression of netrin-1 and its receptors in neuroblastoma (NB), the most frequent extracranial solid tumor of early childhood. The aggressive and metastatic stage 4 NB displays three distinct clinical patterns at presentation and dissemination sites based on patients' ages. Indeed, neonates and infants (<1 yr of age) with stage 4S and stage 4 without 4S features have an overall good prognosis, whereas stage 4 in children (>1 yr of age) shows a poor prognosis. We describe in this paper that, rather than the loss of netrin-1 receptor expression, a large fraction of aggressive NBs has evolved to select a gain of ligand expression that apparently represents a similar selective growth advantage. We therefore propose to use disruption of this selective advantage as an anti-cancer strategy in NB.

## RESULTS

### Netrin-1 is up-regulated in a large fraction of aggressive NB

We focused on stage 4 NB with a specific interest in comparing netrin-1 and its receptors' expression levels between the three distinct clinical patterns of stage 4, based on disease distribution and age of the patients (26). On the one hand, there are the neonates and infants (<1 yr of age) with stage 4S (2–5% of all NB) and the similarly young stage 4 without 4S features, hereafter termed [1yr$^-$] stage 4, who make up 10% of the NB population. On the other hand, there are the stage 4 children (>1 yr of age), comprising 45% of all NBs, who will hereafter be termed [1yr $^+$] stage 4. These three clinical aspects of stage 4 NB differ in their respective malignant behaviors and associated prognoses: good for stage 4S and [1yr $^-$] stage 4 (5-yr event-free survival >80%), and dismal for [1yr $^+$] stage 4 (5-yr event-free survival of ~30%) despite intensive treatment including high-dose chemotherapy and hematopoietic stem cell transplantation (27, 28).

We first analyzed the expression of netrin-1 and its dependence receptors, DCC, UNC5H1, UNC5H2, UNC5H3, and UNC5H4, by quantitative RT-PCR (Q-RT-PCR) in a panel of 102 stage 4 NB tumors including 24 stage 4S and 12 [1yr$^-$] stage 4. As shown in Fig. 1 A, netrin-1 is up-regulated in [1yr$^+$] stage 4 as compared with both stage 4S ($P < 0.05$) and [1yr$^-$] stage 4 ($P < 0.01$). Similar results were obtained when comparing netrin-1 protein level by immunohistochemistry (Fig. 1 B and quantification in Fig. S1 A). Interestingly, netrin-1 is detected mainly in tumor cells and is barely detected in stroma cells (Fig. 1 B and Fig. S1 B). Conversely, netrin-1 dependence receptor expression analysis showed that DCC was only weakly expressed in the different stage 4 NB (Fig. S1 C) as reported (29), whereas UNC5H1, UNC5H2, UNC5H3, and UNC5H4 expression showed no significant differences when comparing [1yr$^-$] versus [1yr$^+$] stage 4 (Fig. 1 C). However, we observed that the different UNC5H receptors are up-regulated specifically in stage 4S (mean increase in UNC5H expression in stage 4S vs. other stage 4 NBs: 2.98-fold, $P < 0.007$), suggesting UNC5H receptors as hallmarks of stage 4S NB. The UNC5H1 and UNC5H4, which show the highest messenger RNA (mRNA) expression, could also be seen at the protein level by immunohistochemistry (Fig. 1 D).

In an attempt to correlate netrin-1 up-regulation with the molecular signature of these tumors, we compared netrin-1 up-regulation and DCC/UNC5H1 levels to the profile of gene expression performed in a small panel of nine stage 4 NBs (30). We failed to detect any correlation between netrin-1 up-regulation or DCC/UNC5H1 levels with the molecular signature of apoptosis or invasion effectors (Fig. S1 D). Considering patients' outcomes, although 38% of [1yr$^+$] stage 4 NBs have selected up-regulation of netrin-1, this event failed to be significantly associated with poor outcome in this aggressive form of the disease (unpublished data). Moreover no association between netrin-1 up-regulation and *MYCN* amplification (MNA) was detected (unpublished data). Thus, netrin-1 up-regulation may be considered as an additional component of the genetic complexity that these tumors display.

Despite a largely favorable prognosis among infants with stage 4 NB (i.e, stage 4S and [1yr$^-$] stage 4) with no MNA, many succumb to the disease. Thus, we assessed whether netrin-1 expression may serve as a prognostic marker for the infants with stage 4 NB. As shown in Fig. 1 E, the overall survival of infants with stage 4S differed markedly based on whether the tumor displayed high levels of netrin-1 expression (netrin-1 high) or low-level expression (netrin-1 low), with the netrin-1 expression threshold being its median expression value in the 102 cases. Indeed, although 100% of the infants survived after 10 yr (including 1 MNA out of 17), when the NB 4S was netrin-1 low, the 5-yr overall survival was only 46% when the NB 4S was netrin-1 high ($P = 0.0109$). Furthermore, 43% of the non-MNA patients with high-level netrin-1 expression died. More generally, when a similar overall survival analysis was performed on all infants with stage 4 NB (i.e. stage 4S and [1yr$^-$] stage 4), a similar dichotomy was observed. Indeed, 5-yr overall survival was found to be 90% for the netrin-1–low infants yet only 48% for netrin-1–high infants ($P = 0.032$; Fig. 1 F). These data suggest that netrin-1 is a potential prognostic marker for aggressiveness in stage 4 NB diagnosed in infants. Whether or not it constitutes an independent prognostic marker of stage 4 NB in neonates and infants deserves to be tested in a larger patient cohort. Nevertheless, these data indicate that a netrin-1 threshold may turn as an alternative determinant for the biological behavior of stage 4 NB in infants, potentially suggesting its involvement in a cell death process of very early childhood neuroblasts, reminiscent of that operating during nervous system development (31).

Netrin-1 high expression is not only detected in 38% of [1yr$^+$] stage 4 and in poor outcome [1yr$^-$] stage 4 primary NB tumors but also in a fraction of NB cell lines mainly derived from stage 4 tumor material (Fig. 2 A and Fig. S2 A). Two human NB cell lines, IMR32 (netrin-1 high) and CLB-Ge2 (netrin-1 low), were evaluated further. In spite of a marked difference in netrin-1 and DCC expression, the UNC5H levels

are similar in IMR32 and CLB-Ge2 cells: UNC5H1, UNC5H3, and UNC5H4 show the highest expression (Fig. 2 B). Specifically, UNC5H1, UNC5H3, and UNC5H4 proteins could be detected at the plasma membrane by confocal analysis (Fig. 2 C). To test the hypothesis that the high netrin-1 mRNA levels detected in IMR32 cells are associated with an autocrine netrin-1 production, we next performed netrin-1 immunohistochemistry on IMR32 and CLB-Ge2 cells. As shown in Fig. 2 D, a netrin-1–specific membrane staining was detected in a homogeneous pattern in IMR32 cells, whereas no specific staining was detected for CLB-Ge2 cells. Confocal analysis further confirmed the presence of netrin-1 at the cell membrane (Fig. 2 E

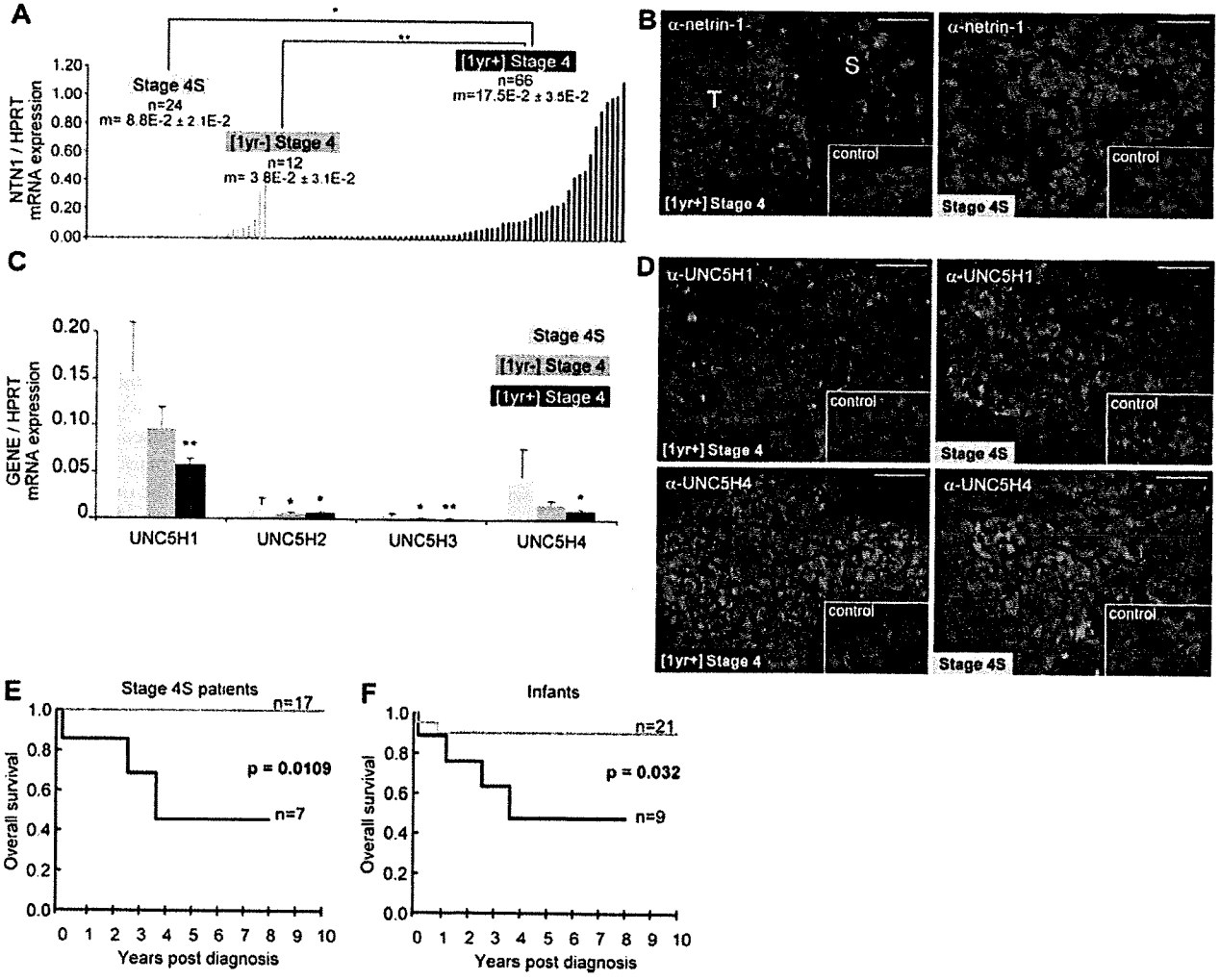


**Figure 1. Netrin-1 up-regulation is detected in aggressive NB.** (A) Netrin-1 mRNA levels in 102 stage 4S ($n$ = 24), [1yr$^-$] stage 4 ($n$ = 12), and [1yr$^+$] stage 4 ($n$ = 66) NBs measured by Q-RT-PCR. HPRT housekeeping gene was used as a control. Mean netrin-1 mRNA expression value for each subgroup is indicated by an "m" value. Mean netrin-1 mRNA levels in stage 4S and [1yr$^-$] stage 4 were, respectively, compared with the mean netrin-1 detected in [1yr$^+$] stage 4. The data were statistically determined using Student's $t$ test compared with levels of [1yr$^+$] stage 4. *, $P < 0.05$; **, $P < 0.01$. Each sample was assessed in two independent experiments. (B) Representative netrin-1 immunohistochemistry on one [1yr$^+$] stage 4 and one stage 4S tumor. Insets show control without primary antibody. Bars, 50 µm. T, tumor cells; S, stromal cells. Netrin-1 antibody specificity is further shown in Fig. 2 D and Fig. S1 B. Immunohistochemistry was performed on four [1yr$^+$] stage 4 and four stage 4S tumors. (C) Mean UNC5H mRNA levels in the different stage 4 NBs. Q-RT-PCR using UNC5H1–4-specific primers was performed. Mean UNC5H1–4 mRNA levels in [1yr$^-$] stage 4 and [1yr$^+$] stage 4 were, respectively, compared with the mean UNC5H1–4 levels detected in stage 4S. Error bars indicate SEM. The data were statistically determined using Student's $t$ test compared with levels of stage 4S. *, $P < 0.05$; **, $P < 0.01$. Samples were analyzed in duplicates for each gene. (D) Representative UNC5H1 and UNC5H4 immunohistochemistries on [1yr$^+$] stage 4 and stage 4S tumors. Insets show control without primary antibody. Bars, 50 µm. Immunohistochemistry was performed on four stage 4 [1yr$^+$] and four stage 4S tumors. (E) Netrin-1 up-regulation is a marker of poor prognosis in stage 4S NB. Overall survival in a panel of 24 infants diagnosed with stage 4S NB with primary tumors showing either netrin-1–low (gray) or netrin-1–high (black) levels. The data was statistically determined using the Kaplan-Meier method. P-value is indicated. (F) Netrin-1 up-regulation is a marker of poor prognosis in infants with NB. Data are presented as in E, with a panel of 30 infants bearing NB.

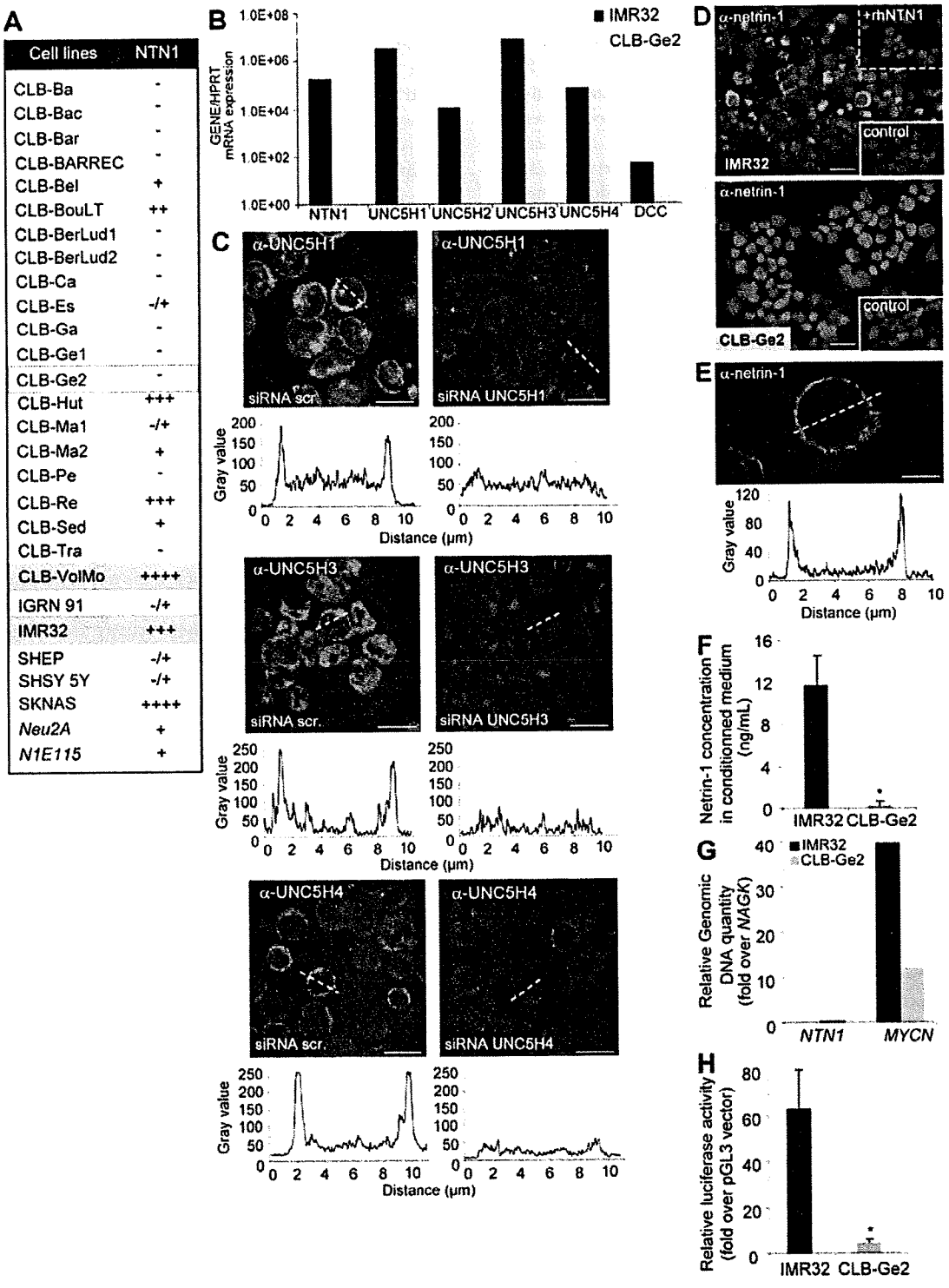


**Figure 2. Netrin-1 up-regulation is detected in NB cell lines.** (A) Netrin-1 expression measured by Q-RT-PCR in a panel of 28 NB cell lines. HPRT housekeeping gene was used as a control. The netrin-1 level is indicated as follows: −, not detectable; −/+, barely detectable; + to ++++, moderate to very high expression. Mouse cell lines are in italics. Cell lines outlined and highlighted in grey are, respectively, netrin-1-low and netrin-1-high cell lines further used in the experiments. (B) Netrin-1 receptor expression in IMR32 and CLB-Ge2 cell lines. DCC/UNC5H Q-RT-PCR was performed on netrin-1-expressing (IMR32) or netrin-1-low (CLB-Ge2) cells using specific primers. Ratio of netrin-1 and netrin-1 receptor expression to the HPRT housekeeping

and Fig. S2 B). To further analyze whether netrin-1 is secreted from IMR32 cells, netrin-1 ELISA assay was used to detect netrin-1 in the conditioned medium. As shown in Fig. 2 F, 11.7 ng/ml netrin-1 was recovered from the conditioned medium of IMR32 cells, whereas no netrin-1 was detected from the conditioned medium of CLB-Ge2 cells. Thus, together these data suggest that the high netrin-1 content observed in aggressive NB could result from an autocrine expression of netrin-1 in NB cells.

As a first approach to apprehend the mechanisms leading to netrin-1 up-regulation in aggressive NB, we analyzed whether netrin-1 gene (*NTN1*) is amplified in IMR32 cells. As shown in Fig. 2 G, although *MYCN* was amplified both in IMR32 and CLB-Ge2 cells compared with the *NAGK* control gene, the *NTN1* gene was not found to be amplified in these two cell lines. We then analyzed whether the increase in netrin-1 expression could be caused by a differential netrin-1 promoter activation. A luciferase reporter gene fused to netrin-1 promoter (32) was then transfected into IMR32 or CLB-Ge2 cells, and luciferase activity was reported to an internal control in each cell line. As shown in Fig. 2 H, netrin-1 promoter activity was 13.8-fold higher in IMR32 cells than in CLB-Ge2 cells, thus supporting the view that netrin-1 up-regulation in NB is related to a gain in netrin-1 promoter activation.

### Netrin-1 up-regulation is a selective advantage for NB cell survival

To investigate whether the netrin-1 autocrine expression observed in IMR32 cells provides a selective advantage for survival, as would be expected from the dependence receptor theory, cell death was analyzed in response to the disruption of this autocrine loop. As a first approach, netrin-1 was down-regulated by RNA interference. As shown in Fig. 3 A, the addition of netrin-1 small interfering RNA (siRNA) to IMR32 cells was associated with a significant reduction in netrin-1 mRNA. This mRNA reduction was associated with a decrease of netrin-1 protein as observed by immunohistochemistry (Fig. 3 B). Although scramble siRNA failed to affect IMR32 cell survival, as measured by trypan blue exclusion, netrin-1 siRNA treatment was associated with IMR32 cell death (Fig. 3 C). In contrast, CLB-Ge2 cell survival was unaffected after netrin-1 siRNA treatment (Fig. 3 C). To determine whether this increase in cell death was in part caused by an increase in apoptotic cell death, caspase-3 activity was measured in response to netrin-1 siRNA treatment. As shown in Fig. 3 D, although significant apoptotic cell death was detected upon netrin-1 siRNA treatment in IMR32 cells, no such effect was observed in CLB-Ge2 cells. A similar proapoptotic effect of the netrin-1 siRNA was observed in CLB-VolMo cells, another netrin-1 high cell line (unpublished data).

### Interference with netrin-1 triggers UNC5H-induced apoptosis in NB cells

As a second approach, we looked for a compound that could interfere with the netrin-1 ability to block DCC/UNC5H proapoptotic activity. We recently reported that the fifth fibronectin type III domain of DCC (DCC-5Fbn; Fig. 4 A), which is located in the DCC ectodomain, interacts with netrin-1 and blocks the ability of netrin-1 to trigger multimerization of DCC and UNC5H receptors. Because multimerization inhibits DCC or UNC5H-induced cell death (unpublished data). DCC-5Fbn antagonizes netrin-1 function, disrupting netrin-1–mediated inhibition of DCC/UNC5H proapoptotic activity. Thus, DCC-5Fbn acts as a trap for netrin-1 survival function. As shown in Fig. 4 (B–D), the addition of DCC-5Fbn, but not the unrelated protein IL3R, triggered IMR32 apoptotic cell death as measured by trypan blue exclusion (Fig. 4 B), caspase-3 activity assay (Fig. 4 C), and terminal deoxynucleotidyl transferase–mediated dUTP-biotin nick end labeling (TUNEL) staining (Fig. 4 D). This effect was specific for netrin-1 inhibition because DCC-5Fbn had no effect on CLB-Ge2 cells, and the addition of netrin-1 ultimately reversed the DCC-5Fbn–induced IMR32 apoptotic cell death (Fig. 4, B–D). Similar results were obtained with the CLB-VolMo cells (Fig. S2 D). To determine whether the ability of DCC-5Fbn to kill NB cells is restricted to established NB cell lines, a surgical biopsy from a tumor with high netrin-1 level (unpublished data) was semidissociated and further incubated with DCC-5Fbn. As shown in Fig. 4 E, DCC-5Fbn triggered cell death as measured by caspase-3 activation, demonstrating that in vitro, disruption of the netrin-1 autocrine loop is associated with NB cell death.

We next investigated whether netrin-1 autocrine expression in NB cells acts as a general cell survival factor, i.e., whether it has a trophic effect similar to that of neurotrophins, or whether it specifically inhibits death induced by

gene is presented. (C) Confocal analysis of UNC5H1, UNC5H3, and UNC5H4 receptor immunostaining in human IMR32 cells. Left and right correspond to IMR32 cells transfected with scramble siRNA and specific siRNA UNC5H, respectively. A fluorescence intensity profile corresponding to the white dashed bar is presented under each panel. Bars, 10 µm. (D) Immunostaining on human IMR32 and CLB-Ge2 cell lines using netrin-1 antibody. Bottom insets show control without primary antibody. Top inset: antibody specificity was tested by adding human recombinant netrin-1. Bars, 50 µm. (E) Confocal analysis of netrin-1 immunostaining on IMR32 cells. A fluorescence intensity profile corresponding to the white dashed bar is presented below. Bar, 5 µm. (F) Quantification of netrin-1 protein secreted in IMR32 and CLB-Ge2 cells conditioned medium by sandwich ELISA assay. Quantification in ng/ml was made according to a dose curve done with recombinant human netrin-1. Data are means of three independent experiments. Error bars indicate SEM. *, $P < 0.05$ using a two-sided Mann-Whitney test compared with level in IMR32 cells. (G) Quantification of *NTN1* and *MYCN* genomic DNA compared with control *NAGK* genomic DNA by PCR, using genomic DNA specific primers for each gene, in IMR32 and CLB-Ge2 cells. (H) Quantification of *NTN1* promoter activity in IMR32 and CLB-Ge2 cells. Both cell lines were transfected with the vector pGL3-NetP-Luc encoding luciferase under the control of *NTN1* promoter. Data presented are normalized on luciferase activity in cells transfected with pGL3 empty vector. Data are means of four independent experiments. Error bars indicate SEM. *, $P < 0.05$ using a two-sided Mann-Whitney test compared with levels in IMR32 cells.

netrin-1 dependence receptors. IMR32 cells were transfected with either a dominant-negative mutant for DCC (DN-DCC) or UNC5H (DN-UNC5H) proapoptotic activity. These dominant-negative mutants of dependence receptors actually encode the intracellular domain of these receptors mutated in their caspase cleavage sites, and these mutants have been shown both in vitro and in vivo to specifically block the proapoptotic activity of their wild-type counterparts (3, 9, 33). Cell death was then analyzed after netrin-1 inhibition by siRNA. Although DN-DCC expression failed to inhibit netrin-1 siRNA-induced IMR32 cell death, expression of DN-UNC5H rendered IMR32 cells resistant to netrin-1 siRNA (Fig. 5 A). To more formally exclude the role in this death process of DCC or of altered forms of DCC that are known to be expressed in IMR32 cells (Fig. S2 C) (34), DCC was down-regulated by a siRNA approach and cell death was induced via netrin-1 siRNA. As shown in Fig. 5 B, DCC siRNA had no effect on cell death per se and failed to inhibit netrin-1 siRNA-induced caspase-3 activation, strengthening the perception that in these cells DCC is not proapoptotic. Neogenin, a DCC homologue, has also been proposed to act as a receptor for netrin-1 (35, 36) even though this is still a matter of controversy (5, 37). We then investigated whether neogenin, which is expressed in IMR32 cells (Fig. S2 C), could be implicated in the IMR32 cell death observed here. Neogenin was down-regulated by a siRNA approach and, as shown in Fig. S3 A, this has no effect on netrin-1 siRNA-mediated IMR32 cell death. Thus, the netrin-1 autocrine loop probably blocks UNC5H-induced IMR32 cell death.

To more specifically address the identity of the UNC5H receptors involved in this cell death induction, we down-regulated the expression of each UNC5H receptor individually (UNC5H1, UNC5H2, UNC5H3, or UNC5H4) by a siRNA approach (Fig. 5 C and Fig. S3 B) while inducing cell death using netrin-1 siRNA (Fig. S3 C). None of the single UNC5H siRNAs was sufficient to inhibit netrin-1 siRNA-mediated IMR32 cell apoptosis, suggesting some redundancy in UNC5H-induced cell death (Fig. 5 D). However, when combinations of siRNAs were used, we observed that combined silencing of the four UNC5H receptors was sufficient to fully inhibit the death triggered by netrin-1 autocrine loop disruption (Fig. 5 D), whereas the same combination of siRNAs had no effect on CLB-Ge2 cell survival (Fig. S3 D). The respective importance of UNC5H receptors in netrin-1 siRNA-induced cell death was then assessed by the different combination of two or three siRNAs; the combination of UNC5H1, UNC5H3, and UNC5H4 siRNAs was the only one to fully block cell death (Fig. 5 E). Thus, in agreement with the level of UNC5H receptors expressed in IMR32 cells, it appears that disruption of the netrin-1 autocrine survival loop triggers UNC5H-induced cell death. Moreover,

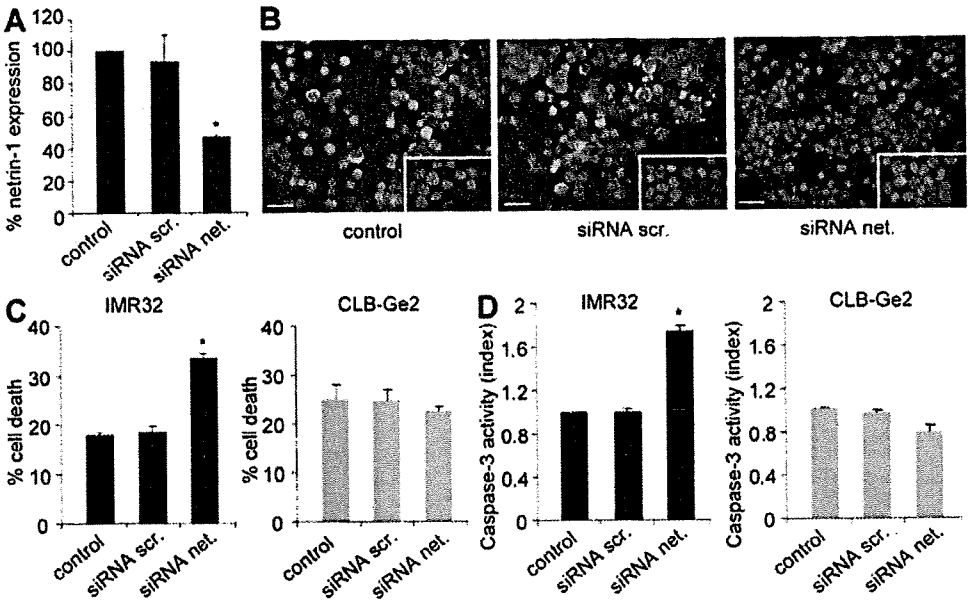


**Figure 3. Down-regulation of netrin-1 autocrine loop by siRNA triggers NB tumor cell death.** (A) Analysis of netrin-1 expression using Q-RT-PCR in nontransfected (control) IMR32 cell line or 24 h after transfection with scramble siRNA (siRNA scr.) or with netrin-1 siRNA (siRNA net.). Data are means of three independent experiments. Error bars indicate SEM. *, $P < 0.05$ using a two-sided Mann-Whitney test compared with levels in control.
(B) Immunostaining on IMR32 cell line using netrin-1 antibody in the absence of transfection (control) or 24 h after transfection with scramble siRNA or netrin-1 siRNA. Note that the general caspase inhibitor z-VAD-fmk was added to avoid cell death induced by netrin-1 siRNA. Insets show control without primary antibody. Bars, 50 μm. (C and D) Cell death induction in IMR32 and CLB-Ge2 cell lines was quantified in nontransfected cells (control) or after transfection with either scramble siRNA or netrin-1 siRNA using trypan blue exclusion assay (C) or relative caspase-3 activity assay (D). Data are means of four independent experiments. In C and D, error bars indicate SEM. *, $P < 0.05$ calculated using a two-sided Mann-Whitney test compared with level of control.

UNC5H1, UNC5H3, and UNC5H4 are the receptors involved in this proapoptotic effect.

Furthermore, in IMR32 cells, the proapoptotic serine threonine kinase DAP kinase (DAPK), which is shown to be required for UNC5H-induced cell death, exhibited a loss of its inhibitory autophosphorylation (38) upon DCC-5Fbn treatment (Fig. 5 F) or netrin-1 siRNA transfection (Fig. 5 G). Accordingly, autophosphorylation was restored by a treatment with excess netrin-1 or by a combination of UNC5H1, UNC5H3, and UNC5H4 siRNAs. Moreover, the transfection of the antiapoptotic protein BCL-2 was sufficient to inhibit netrin-1 siRNA-induced cell death but did not inhibit DAPK dephosphorylation, hence suggesting that DAPK activation is not a result of cell death but is specifically engaged by UNC5H after netrin-1 inhibition (unpublished data).

### Interference with netrin-1 inhibits NB progression and dissemination

We next assessed whether in vivo modulation of netrin-1 could be used to limit/inhibit NB progression and dissemination. An elegant chicken model has been developed in which graft of NB cells in the chorioallantoic membrane (CAM) of 10-d-old chick embryos recapitulates both tumor growth at a primary site, i.e., within the CAM, and tumor invasion and dissemination at a secondary site, metastasis to the lung (Fig. 6 A). In a first approach, IMR32 or CLB-Ge2 cells were loaded in

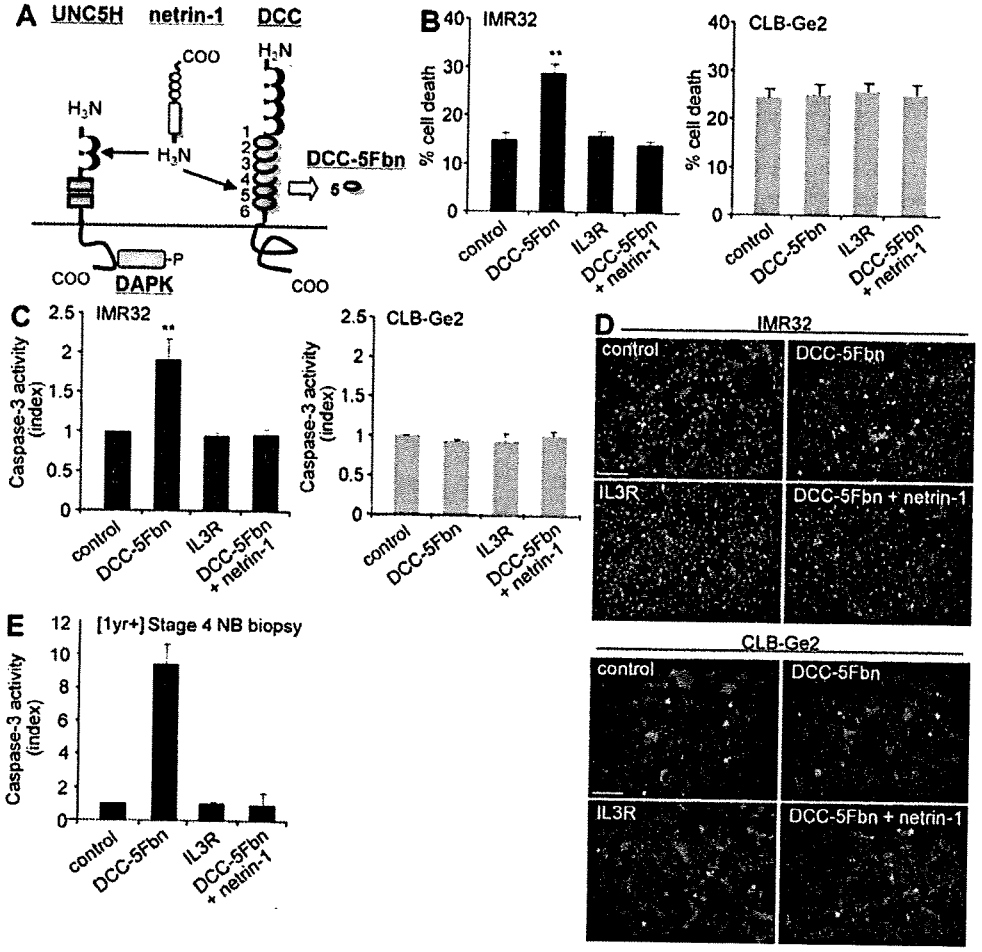


**Figure 4. Disruption of netrin-1 autocrine loop by a decoy receptor fragment triggers NB tumor cell death.** (A) Scheme representing netrin-1 and its receptors DCC and UNC5H and the fifth fibronectin type III domain of DCC (DCC-5Fbn) used to induce cell death. The downstream effector DAPK implicated in UNC5H-induced cell death is also represented. (B–D) Quantitative analysis of cell death in IMR32 and CLB-Ge2 cell lines treated with 1 μg/ml DCC-5Fbn, with or without addition of netrin-1 in excess (150 ng/ml) to reverse the effect of DCC-5Fbn. A negative control was also performed by adding an unrelated IL3R peptide produced in the same condition as DCC-5Fbn. Cell death was quantified by trypan blue exclusion assay (B) while apoptosis was monitored by measuring relative caspase-3 activity (C) or by TUNEL staining (D). Bars, 100 μm. In D, TUNEL staining was performed on three independent experiments. (E) Effect of DCC-5Fbn on fresh [1yr+] stage 4 NB. Tumoral cells were directly resuspended from the surgical punction and were plated for 24 h in presence of treatment. In B and C, data are means of six independent experiments. In E, data are means of two independent experiments. Error bars indicate SEM. **, $P < 0.01$ calculated using a two-sided Mann-Whitney test compared with level of control.

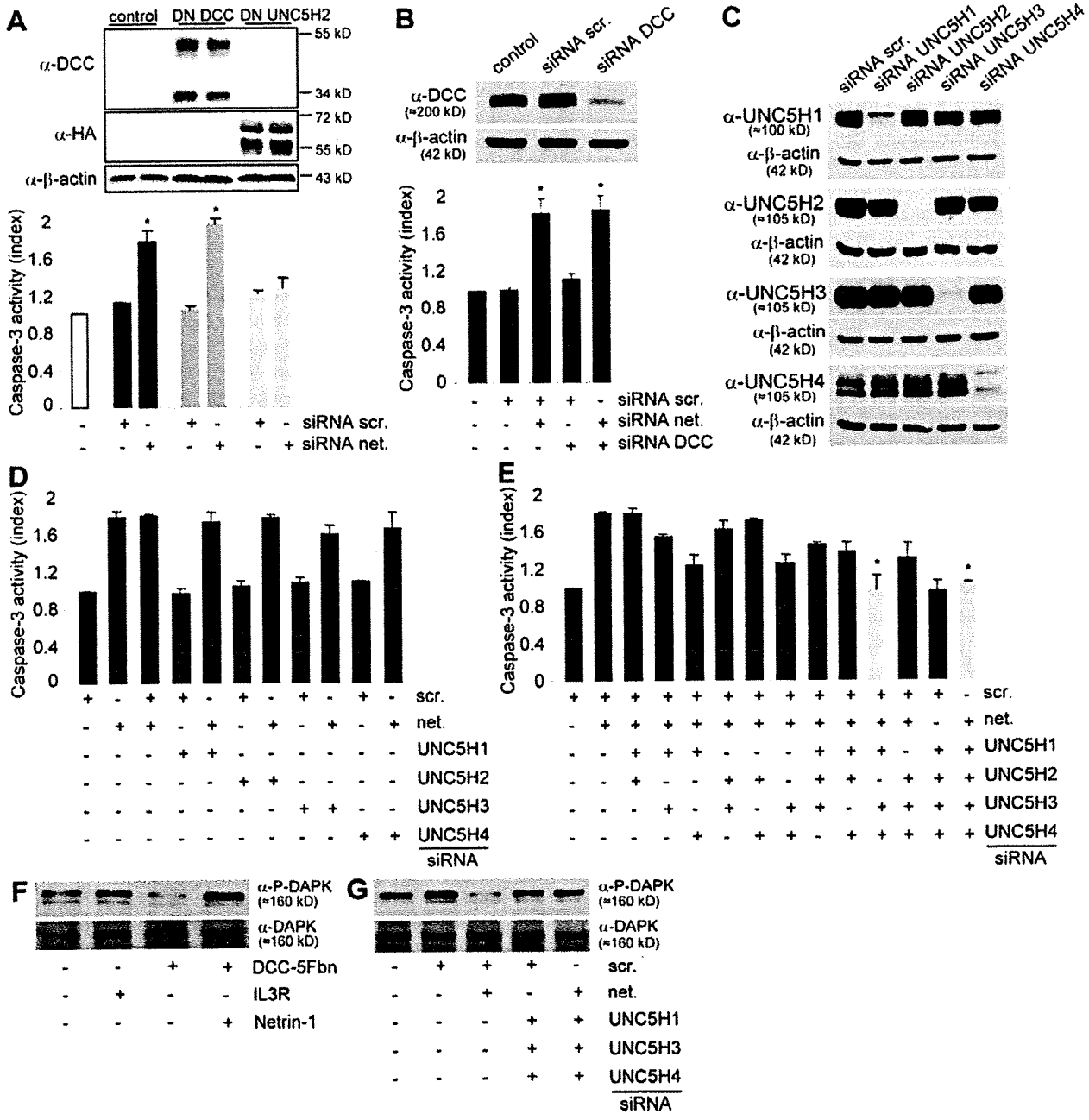


**Figure 5. NB tumor cell death occurs via UNC5H/DAPK proapoptotic signaling.** (A) Quantification of cell death in IMR32 cells transfected with either a dominant-negative mutant for DCC proapoptotic activity (DN-DCC) or a dominant-negative mutant for UNC5H proapoptotic activity (DN-UNC5H). Top: DN-DCC and DN-UNC5H proteins expression were analyzed by Western blot. Bottom: cell death was quantified by measuring relative caspase-3 activity after scramble or netrin-1 siRNA transfection. SEM are indicated. Data are means of three independent experiments. *, $P < 0.05$ calculated using a two-sided Mann-Whitney test compared with level of control. (B) Quantification of cell death in IMR32 cells transfected with either a scramble siRNA or a netrin-1 siRNA together or not with a DCC siRNA. Top: DCC siRNA efficiency was verified by Western blotting on HEK293T cells transfected with pCR-hDCC together with scramble or DCC siRNA. Bottom: cell death was quantified by measuring relative caspase-3 activity. Data are means of three independent experiments. SEM are indicated. *, $P < 0.05$ calculated using a two-sided Mann-Whitney test compared with level of control. Similar results were obtained when neogenin or MYCN were down-regulated (Fig. S3 A). (C) Analysis of specificity and efficiency of each UNC5H siRNA by Western blot in HEK293T cells transfected with UNC5H1, H2, H3, or H4 encoding vector together with each UNC5H siRNA. (D and E) Quantification of cell death in IMR32 cells transfected with either a scramble siRNA or a netrin-1 siRNA together with various combinations of UNC5H siRNA, i.e, one UNC5H (D) or two or four UNC5H (E). Apoptosis was monitored by measuring relative caspase-3 activity. The use of combined UNC5H1, UNC5H2, UNC5H3, and

10-d-old CAM and embryos were treated on days 11 and 14 with PBS or DCC-5Fbn. 17-d-old chicks were then analyzed for primary tumor growth and metastasis to the lung. As shown in Fig. 6 (B and C), specifically in CAMs grafted with IMR32 but not with CLB-Ge2 cells, DCC-5Fbn significantly reduced primary tumor size. This size reduction was associated with increased tumor apoptosis, as shown by an increased caspase-3 activity in the tumor lysate (Fig. 6 D). More importantly, DCC-5Fbn also reduced lung metastasis formation, as shown in Fig. 6 E. Similar results were obtained when CAM-grafted embryos were treated with netrin-1 siRNA (unpublished data). To next assess whether DCC-5Fbn could also induce the regression of metastatic lesions, IMR32 cells were CAM grafted and DCC-5Fbn (or PBS) treatment started after metastasis to the lung is known to occur, i.e., treatments were performed on days 14 and 15 because pulmonary metastases are routinely detectable at day 13. As shown in Fig. 6 F, pulmonary metastases were markedly reduced, suggesting that DCC-5Fbn not only inhibits tumor dissemination but also induces regression of metastatic lesions at the secondary site.

As a second in vivo approach, we used the IGR-N-91 model derived from a BM metastasis of human MYCN-amplified stage 4 NB. When subcutaneously xenografted into nude mice, IGR-N-91 cells gave rise to different tumor cell lines derived from the *nude* mouse primary tumor xenograft (PTX) or from disseminated metastatic foci into BM, blood, and myocardium (Myoc) of the animal (39). It is of interest that although the parental IGR-N-91 and the cell line derived from the PTX show no or very low netrin-1 expression, the different cell lines derived from secondary localizations showed a marked expression of netrin-1 both at the RNA level (Fig. 7 A) and at the protein level (Fig. 7 B). When cell death was investigated in these different cell lines upon treatment with DCC-5Fbn, a direct correlation was observed between the level of netrin-1 and cell susceptibility to DCC-5Fbn (Fig. 7 C). Specifically, although PTX cells failed to undergo cell death upon DCC-5Fbn treatment, this treatment triggered netrin-1–high Myoc cell death (Fig. 7 C). This observation supports the overall view that gaining netrin-1 dependence receptor resistance, via an autocrine netrin-1 expression in the case of the IGR-N-91 model, likely promotes NB tumor cell survival outside of the primary tumor site. To test whether this netrin-1 expression may then be used as a target to inhibit metastasis in vivo, Myoc and PTX cells were injected intravenously into *nude* mice and lung colonization was quantitated after daily intraperitoneal treatment with PBS or DCC-5Fbn. Although lung colonization was not reduced upon DCC-5Fbn treatment in PTX-injected mice (not depicted), a significant decrease in lung colonization was detected in DCC-5Fbn–treated Myoc-injected mice (Fig. 7 D). Thus, in both chick and mouse models, disruption of the netrin-1 autocrine loop inhibited or completely prevented the dissemination of netrin-1–expressing NB cells.

## DISCUSSION

Together, the data obtained in the chick and mouse models described in the previous sections, in NB cell lines, and in the human pathology all support the view that a fraction of NB shows an autocrine production of netrin-1. This elevated netrin-1 level likely confers a selective advantage acquired by the cancer cell to escape netrin-1 dependence receptor–induced apoptosis and, consequently, to survive in settings of environmental absence or limitation of netrin-1. It is therefore interesting to note that not only NB but also other neoplasms associated with poor prognosis, for example, metastatic breast cancer and pancreatic cancer, also express high levels of netrin-1 (33, 40), suggesting that netrin-1 up-regulation may be a common feature for several aggressive cancers. From a mechanistic point of view, in a large fraction of NB, this autocrine expression of netrin-1 probably inhibits UNC5H-induced cell death. However, because DCC has been shown to display reduced expression in NB and because this reduction has been associated with NB aggressiveness in human NB (29), it is tempting to speculate that netrin-1 up-regulation can also, in some NB, inhibit DCC-induced apoptosis. Interestingly, this netrin-1 up-regulation appears to block a death signal involving the serine threonine DAPK, whose activity is regulated via its autophosphorylation. It is therefore of interest to note that DAPK was described to be a negative regulator of tumor progression and, more specifically, of metastasis (41). Thus, it can be suggested that a fraction of low netrin-1–expressing NB may have selected a loss of function of DAPK for survival. This would be compatible with the finding that metastasis in NB is associated with a loss of caspase-8, a selective advantage which provides survival to NB cells by inhibiting the proapoptotic signaling of the dependence receptor integrin $\alpha 3\beta 1$ (42).

It is then interesting to wonder why such a large fraction of aggressive NBs have selected a gain of netrin-1 rather than a loss of the netrin-1 dependence receptor death pathways. A possible explanation is that netrin-1 expression not only confers a gain in survival, but may also lead to enhancement of non-apoptotic signaling mediated by netrin-1 receptors. Netrin-1 was indeed shown to bind a complex that includes some integrins (43). These integrins regulate cell migration and invasiveness and, thus, may play a role in cancer progression. Netrin-1 was also proposed to play a role in angiogenesis, although whether netrin-1 is proangiogenic or antiangiogenic is controversial (44–47) and this effect on angiogenesis may increase NB metastases development. It is also of interest to note that NB is a complex disease that originates from migrating neural crest cells. Netrin-1 up-regulation may then be implicated in

UNC5H4 or UNC5H1, UNC5H3, and UNC5H4 siRNAs, leading to the absence of death induced by netrin-1 siRNA, are presented in gray. Data are means of three independent experiments. Error bars indicate SEM. *, $P < 0.05$ calculated using a two-sided Mann-Whitney test compared with level of control. (F and G) Immunodetection of phosphorylated DAPK (P-DAPK) in IMR32 cells either treated with DCC-5Fbn (F) or transfected with netrin-1 siRNA alone or with UNC5H1, H3, and H4 siRNAs (G). In F and G, immunodetection was performed on three independent experiments.

the main function played by netrin-1 during nervous system development that is neuronal navigation. Along this line, netrin-1 and DCC have been shown to play an important role during neural crest cell migration (48), and it is then tempting to suggest that the gain in netrin-1 expression also promotes NB cell migration.

As different types of stage 4 NBs are distinguished, not only by the age of the children but also by the tissues in which metastases are found, one may wonder about the implication of netrin-1 produced in the normal tissues in which the tumor cells spread, and this would be interesting to explore. In particular, it would be interesting to evaluate whether, according to the classical "seed and soil" theory for metastasis (for review see reference 18), netrin-1 expression in specific tissues may favor metastasis development more specifically in these tissues. It is also intriguing

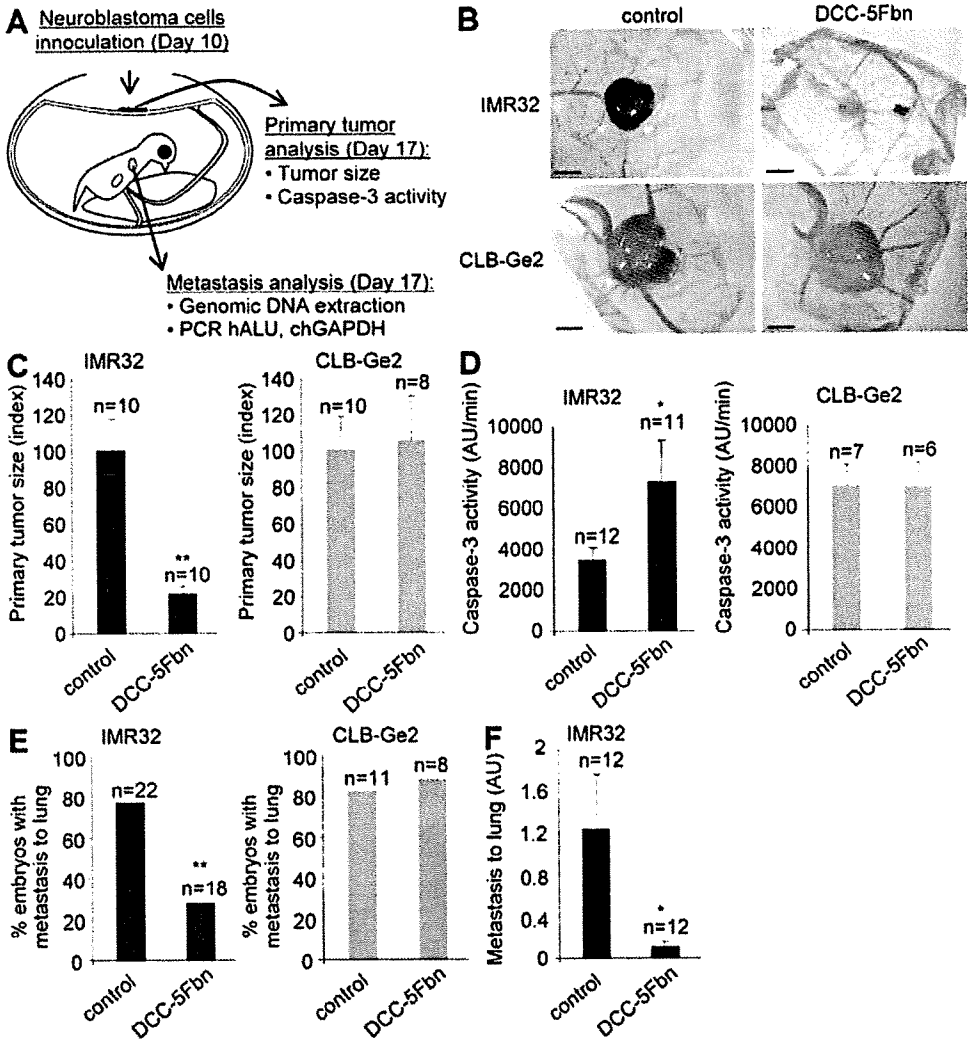


**Figure 6. Disruption of netrin-1 autocrine loop inhibits NB progression and dissemination in a chick model.** (A) Schematic representation of the experimental chick model. IMR32 or CLB-Ge2 cells were grafted in CAM at day 10 and DCC-5Fbn or PBS was injected on days 11 and 14. Tumors and lungs were harvested on day 17. (B–D) Effect of DCC-5Fbn on primary tumor growth and apoptosis. (B) Representative images of IMR32 (top) or CLB-Ge2 (bottom) primary tumors formed on CAM treated either with DCC-5Fbn (right) or PBS (left). Bars, 2 mm. (C) Quantitative analysis showing the mean primary tumor size. (D) Caspase-3 activity was determined in the primary tumor lysates from DCC-5Fbn/PBS-treated IMR32 or CLB-Ge2–grafted embryos. (E) Effect of DCC-5Fbn on lung metastasis. Percentage of embryos with lungs invaded by human IMR32 or CLB-Ge2 cells after two injections (days 11 and 14) of either DCC-5Fbn or PBS was performed as described in the Materials and methods. (F) Effect of DCC-5Fbn on lung metastasis regression. Quantification of lung metastasis in embryos CAM grafted with IMR32 cells and treated after metastasis formation (days 14 and 15) with DCC-5Fn or PBS. The number of embryos studied in each condition is indicated above the graphs and results are from three independent experiments. In C–F, errors bars indicate SEM. C–F: *, $P < 0.05$; **, $P < 0.005$ calculated using a two-sided Mann-Whitney test compared with level of control. E: **, $P < 0.005$ calculated using a Chi-squared test.

to note that others have shown that in some particular cell lines, netrin-1 is able to promote apoptosis rather than inhibit apoptosis (49), so that the view of netrin-1 up-regulation being only a survival-selective advantage to block apoptosis via dependence receptors is probably only part of the overall regulatory mechanisms that links NB, netrin-1, and its receptors.

The observation that low levels of netrin-1 in NB correlate with good outcome is of clinical interest, in particular in NB diagnosed in neonates and infants. Indeed, low netrin-1 expression predicts long-term survival in infants (100% in 4S stage and 90% in infants in general) in a type of pathology in which therapeutic management is highly dependent on presentation and MNA (50, 51). This is particularly true with

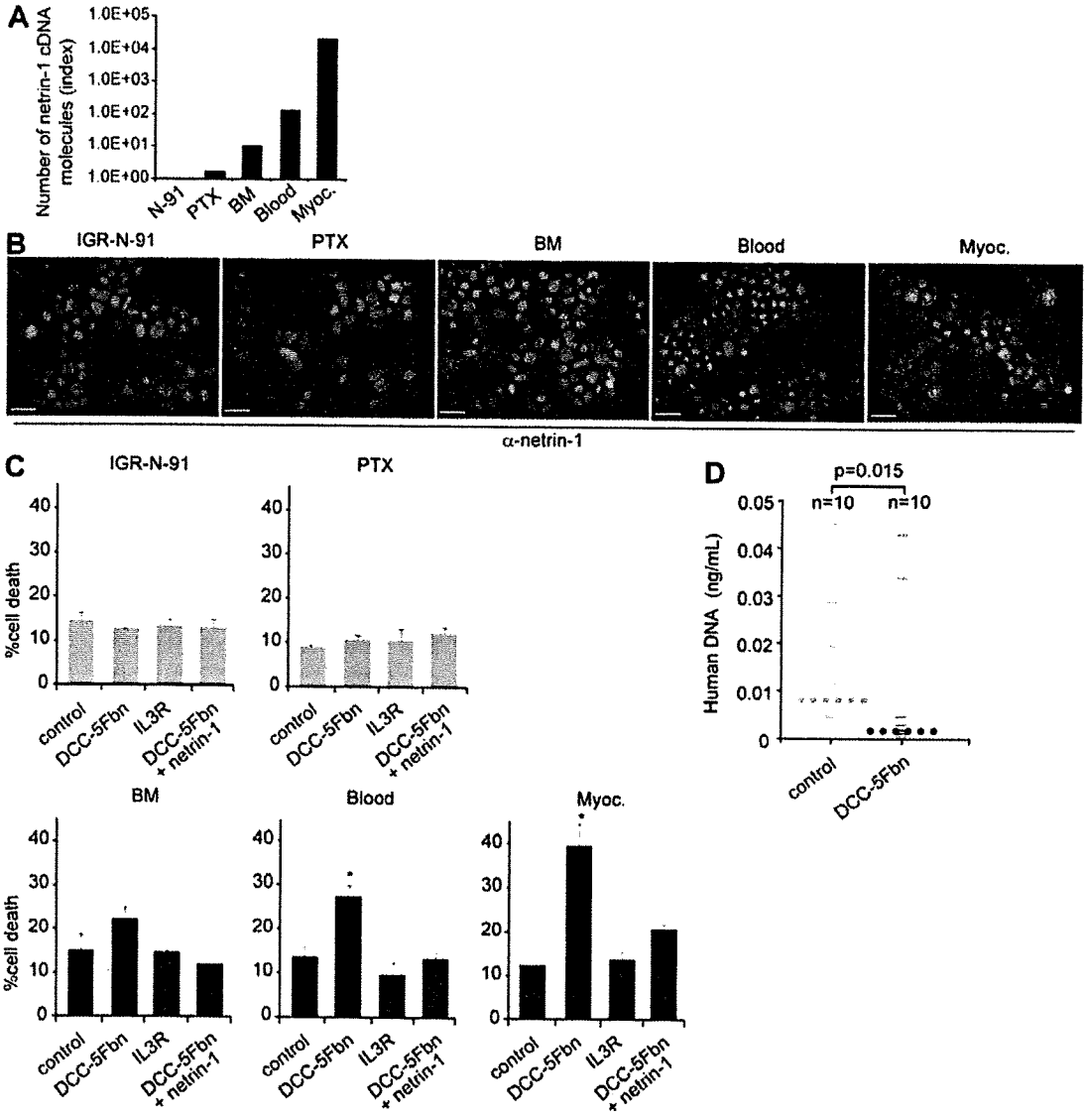


**Figure 7. Disruption of netrin-1 autocrine loop inhibits NB dissemination in a mouse model.** (A) Analysis of netrin-1 expression using Q-RT-PCR in IGR-N-91 cell line and the IGR-N-91–derived cell lines PTX, BM, Blood, and Myoc. Note that although PTX cells fail to express netrin-1, netrin-1 mRNA is highly expressed in Myoc cells. (B) Immunostaining on IGR-N-91 cells and the different derived cell lines PTX, BM, Blood, or Myoc using netrin-1 antibody. Bar, 50 µm. (C) Cell death was quantified in IGR-N-91, PTX, BM, Blood, or Myoc cell lines treated or not with DCC-5Fbn, with or without addition of netrin-1 in excess to reverse the effect of DCC-5Fbn. A negative control was also performed by adding an unrelated IL3R peptide produced in the same condition as DCC-5Fbn. Data are means of three independent experiments. Errors bars indicate SEM. *, $P < 0.05$, calculated using a two-sided Mann-Whitney test compared with level of control. (D) Quantification of lung colonization in PTX or Myoc cells in i.v injected mice treated with PBS or DCC-5Fbn for 22 d. Quantification was performed as described in the Materials and methods. Large bars indicate the median values for both groups. P-value was calculated using a two-sided Mann-Whitney test compared with level of control.